Accepted Manuscript

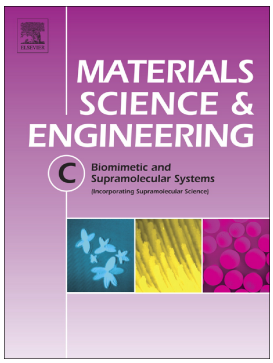

Understanding and augmenting the stability of therapeutic nanotubes on anodized titanium implants

Tao Li, Karan Gulati, Na Wang, Zhenting Zhang, Sašo Ivanovski

PII: S0928-4931(17)34273-X
DOI: doi:10.1016/j.msec.2018.03.007
Reference: MSC 8428

To appear in: *Materials Science & Engineering C*

Received date: 30 October 2017
Accepted date: 13 March 2018

Please cite this article as: Tao Li, Karan Gulati, Na Wang, Zhenting Zhang, Sašo Ivanovski , Understanding and augmenting the stability of therapeutic nanotubes on anodized titanium implants. The address for the corresponding author was captured as affiliation for all authors. Please check if appropriate. Msc(2017), doi:10.1016/j.msec.2018.03.007

Understanding and Augmenting the Stability of Therapeutic Nanotubes on Anodized Titanium Implants

Tao Li [a,b,c], Karan Gulati ✉ [a,b,d], Na Wang [c], Zhenting Zhang [c] and Sašo Ivanovski ✉ [a,b,d]

[a] School of Dentistry and Oral Health, Griffith University, Gold Coast, QLD, Australia

[b] Menzies Health Institute Queensland (MHIQ), Griffith University, Gold Coast, QLD, Australia

[c] Department of Prosthodontics, School of Stomatology, Capital Medical University, Beijing, People's Republic of China

[d] School of Dentistry, University of Queensland, Herston, QLD, Australia

✉Corresponding Author

Prof. Sašo Ivanovski (s.ivanovski@uq.edu.au) and Dr. Karan Gulati (k.gulati@uq.edu.au)

School of Dentistry, University of Queensland, 288 Herston Road, Herston QLD 4006, Australia

Keywords: anodization, implants, mechanical stability, titanium, titania nanotubes

Abstract

Titanium is an ideal material for orthopaedic and dental implants, and hence a significant amount of research has been focused towards augmenting the therapeutic efficacy of titanium surfaces. More recently the focus has shifted to nano-engineered implants fabricated via anodization to generate self-ordered nanotubular structures composed of titania (TiO_2). These structures (titania nanotubes/TNTs) enable local drug delivery and tailorable cellular modulation towards achieving desirable effects like enhanced osseointegration and antibacterial action. However, the mechanical stability of such modifications is often ignored and remains underexplored, and any delamination or breakage in the TNTs modification can initiate toxicity and lead to severe immuno-inflammatory reactions. This review details and critically evaluates the progress made in relation to this aspect of TNT based implants, with a focus on understanding the interface between TNTs and the implant surface, treatments to augment the mechanical stability and the advanced mechanical testing within the bone micro-environment *ex vivo* and *in vivo*. This review article extends the existing knowledge in this domain of TNTs implant technology and will enable improved understanding of the underlying parameters that contribute towards mechanically robust nano-engineered implants that can withstand the implant surgical placement and the load bearing forces experienced at the bone/implant interface.

1. Introduction

Titanium and its alloys are clinically preferred biomaterials for bone implants due to their superior biocompatibility and corrosion resistance [1]. Titanium (Ti) has been extensively used for manufacturing hard tissue implants to replace and/or correct missing or diseased tissues in clinical applications such as total joint replacements, fracture fixation (plates, nails or screws) and dental implants. It is reported that over 327,000 hip replacements were performed in 2009 in the United States alone, and the orthopaedic implant market is estimated at $33 billion with projected increases of 7.1% per year [2, 3]. Notwithstanding relatively high success rates, around 4.1%~7% implants face challenges mainly due to excessive inflammation, poor osseointegration and bacterial infection, which can result in complete implant failure requiring revision surgery [4, 5]. These challenges may be addressed by augmenting the bioactivity of Ti based implants via surface modification. This can be achieved by altering the surface topography in the macro, micro and nanoscales [6].

Macroscale (millimetres to micrometres) directly relates to implant geometry, with threaded screws and macro-porous surfaces being commonly utilized in the clinic. Reports have demonstrated that macro-roughness features lead to an increase both in early bone apposition and implant fixation by improving mechanical interlocking between the macro-rough features and surrounding bone [7, 8]. However, the direct bone-implant contact can be maximized by micro-roughness (1–10 micrometres), which can be produced by sandblasting, acid etching, plasma spraying and other surface modification techniques [9]. Furthermore it has been theoretically calculated that the ideal implant surface features at the micro-scale should be 1.5 μm long and 3-5 μm wide [10, 11]. Despite numerous studies demonstrating that micro-roughness augment bone-to-implant contact and torque removal resistance [12, 13], it is noteworthy that the initial fate of host tissues and cells is not directly affected by microscale surface roughness [14]. Rather, biomolecular interactions, protein adsorption and bone cell behaviour can be influenced by nanostructures (1-100 nm) [15-17]. In this context, nanoscale topography has been regarded as a promising surface modification strategy for Ti based implants [18].

Recently, nanoscale features (TiO_2 nanopores or nanotubes) generated by self-ordering electrochemical anodization (EA) technique, have drawn considerable attention as a means of improving the bioactivity and therapeutic potential of conventional Ti implants [19]. EA enables cost-effective fabrication of well-ordered titania nanotubes (TNTs) on titanium

surfaces with great control over TNTs characteristics, achievable by varying the anodization parameters [20]. The influence of TNTs on cellular functions (mesenchymal stem cells, hematopoietic stem cells, endothelial cells, osteoblasts, and osteoclasts) including adhesion, proliferation and differentiation has been extensively investigated in the context of bone/dental implant applications [21]. A critical finding is that nanotube dimensions and other characteristics (wettability, crystal structure, loading of drugs/proteins, etc.) significantly dictates cell functionality [22]. Furthermore, due to the geometry of TNTs (resembling tiny test tubes, open at top, closed at bottom), they can act as a drug reservoir for the local delivery of drugs (antibiotics, proteins, anti-inflammatory or anti-cancer drugs) directly inside the implant micro-environment, with the ultimate aim of improving the therapeutic efficacy of conventional implants [23, 24].

Despite significant advancements achieved in the domain of TNTs modified implants, many research gaps are challenging the successful translation of TNTs from research to clinical testing and integration into the commercial implant market. For example, the critical issue of the mechanical properties and stability of TNTs remains underexplored. The mechanical characteristics of a titanium implant and its therapeutic extensions such as TNTs, including elastic modulus, hardness and fracture strength, play a decisive role in its long-term success, especially in bone/dental implant scenarios requiring surgical placement and survival in load bearing conditions. Indeed, in the presence of cracks and delamination due to mechanical stress and abrasion, severe host immune-inflammatory reactions may occur, which can lead to complete implant failure. Highlighting this research gap, in this review article we elaborate on the underlying factors determining the mechanical stability of TNTs based anodized Ti implants (Fig. 1). This review article details the in-depth understanding of the interface between TNTs and the Ti implant substrate, identifying issues that may affect mechanical stability and integrity. Furthermore, it incorporates a critical discussion of the various strategies used to augment mechanical stability, as well as implantation studies performed *ex vivo* and *in vivo* highlighting the survival of TNTs based implants.

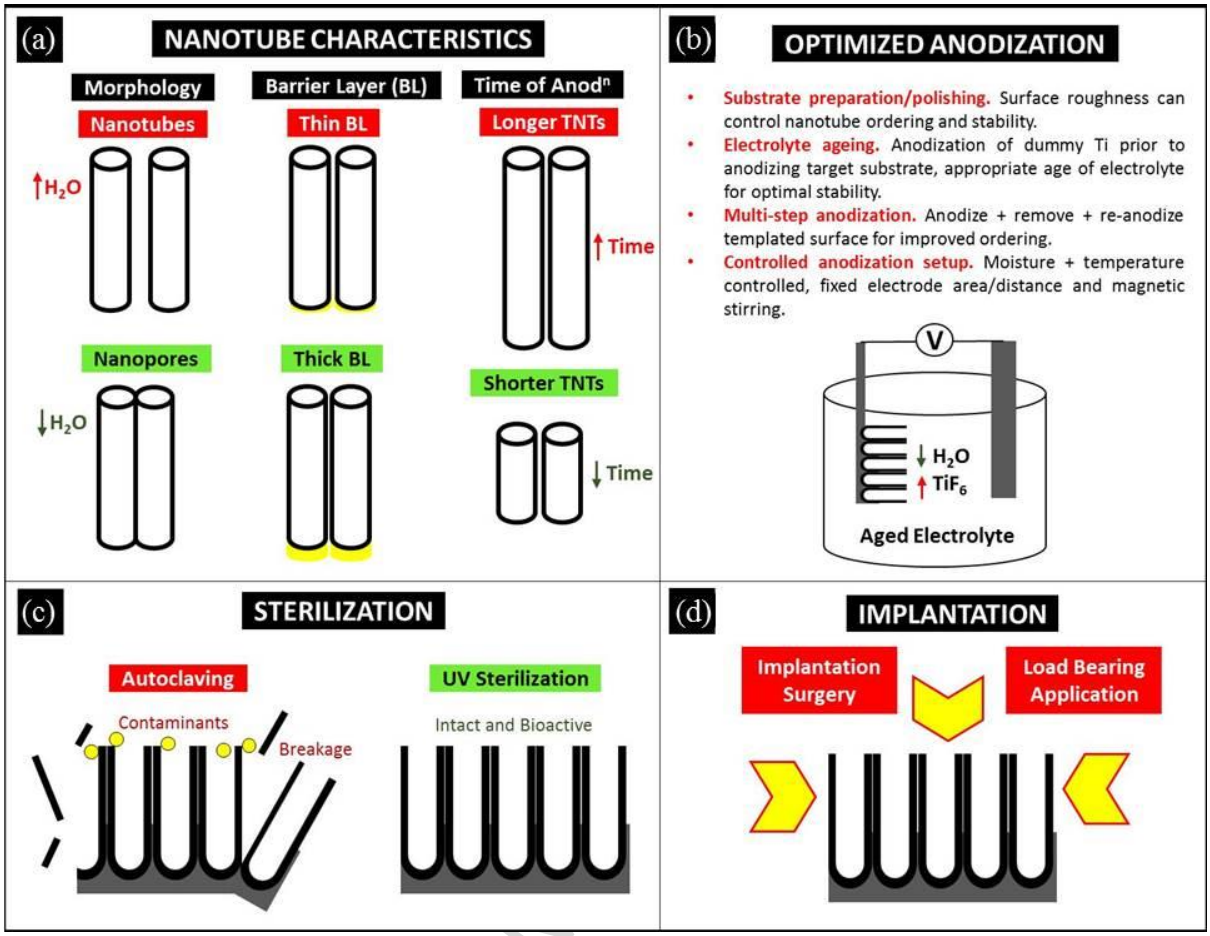

Figure 1 Schematic representation of the parameters influencing the mechanical stability of titania nanotubes (TNTs) fabricated via electrochemical anodization.

2. Understanding the Interface between Nanotubes and Titanium Substrate

In 1999, pioneering work by Zwilling et al. reported the fabrication of self-organized TNTs on Ti via EA in HF based electrolytes [25]. This first generation of TNTs could be fabricated up to a limited length of around 500nm, with considerable sidewall inhomogeneity [26]. Future research focused on generating TNTs with lengths up to several micrometers and extremely smooth homogenous sidewalls by varying the pH values, anodizing voltage/time and introducing organic electrolytes [27-29]. However, for the orthopaedic/dental implant setting, which is continuously under load bearing, the stable adhesion of bioactive or drug incorporated TNTs to the underlying Ti implant substrate is essential to ensure long term success in what is often compromised bone micro-environment. This section of the review will provide an overview of the fabrication mechanisms and critical factors affecting TNTs geometry and composition for an

improved understanding of the factors that may influence the mechanical stability and the interface between nanotubes and the implant substrate (Fig. 1).

2.1 Mechanism of Electrochemical Anodization of Ti

Briefly, EA is performed by exposing a two-electrode system to DC voltage in an appropriate fluoride-based electrolyte, with Ti as the anode and platinum/Ti as the cathode. Under optimized conditions, the as-fabricated TNTs are vertically oriented on the Ti surface and homogeneously ordered with a closed bottom and open top (Fig. 1). The growth mechanism of self-ordered TNTs is the result of three simultaneous reactions, which can also be related to different regions observed in the current–time curves as shown in Fig. 2(a). The formation of TNTs is schematically depicted in Fig. 2(b). The anodization process starts when Ti is oxidized to Ti^{4+} [equation (i)] to form a compact TiO_2 layer [equation (ii)] accompanied by the transport of Ti^{4+} ions outward and O^{2-} ions inward with the assistance of an electric field.

(i) $Ti \rightarrow Ti^{4+} + 4e^-$

(ii) $Ti + 2H_2O \rightarrow TiO_2 + 4H^+ + 4e^-$

Anodic oxidation processes typically follow equation (iii), where U is the applied voltage and d represents the thickness of the oxide. That is, the field keeps on decreasing with the increase in film thickness until it is not sufficient to promote ion transport and the finite film thickness forms.

(iii) $F=U/d$

The presence of fluoride ions can significantly influence the anodization process [20]. On one hand, fluoride ions chemically dissolve TiO_2 or directly react with Ti^{4+} arriving at the oxide–electrolyte interface to form water-soluble $[TiF_6]^{2-}$ complexes [equations (iv), (v)]. The ability to form these soluble complexes results in the permanent chemical dissolution of compact TiO_2, thereby leading to the transformation of the compact layer to hollow porous and tubular structures. On the other hand, the small ionic size makes fluoride ions easier than O^{2-} to get through the TiO_2 layer, thus forming an approximately 15 nm thick fluoride-rich layer at the metal-oxide interface [28]. This layer is very important to nanotube growth and significantly influences the adherence of TNTs to the Ti substrate, which will be discussed in section 2.2.

(iv) $TiO_2 + 6HF \rightarrow [TiF_6]^{2-} + 2H_2O + 2H^+$

(v) $Ti^{4+} + 6F^- \rightarrow [TiF_6]^{2-}$

According to the typical current-time curve for self-organized TNTs in aqueous electrolyte with intermediate fluoride concentrations (0.1–1 wt %), the EA process can be divided into three stages [20, 29]. In the first stage, the current initiates exponential decay due to the formation of a compact oxide barrier layer. In stage two, random nanopores start to grow which increases the active area, and thereby the current rises. In stage three, the current density reaches a steady level which promotes the self-organization of TNTs. The tubes grow continually with time until the etching rate at the top of the tube is equivalent to the formation rate at the bottom, as depicted in Fig. 2(c) [30]. It is noteworthy that the TNTs morphology turns into a v-shape with extended anodization time since chemical dissolution occurs at the entire tube length, which means that the walls of the nanotube tops are significantly thinner than the bottoms [31]. In the following sections we will have a look at the various EA parameters that can contribute towards the fabrication of robust TNT structures.

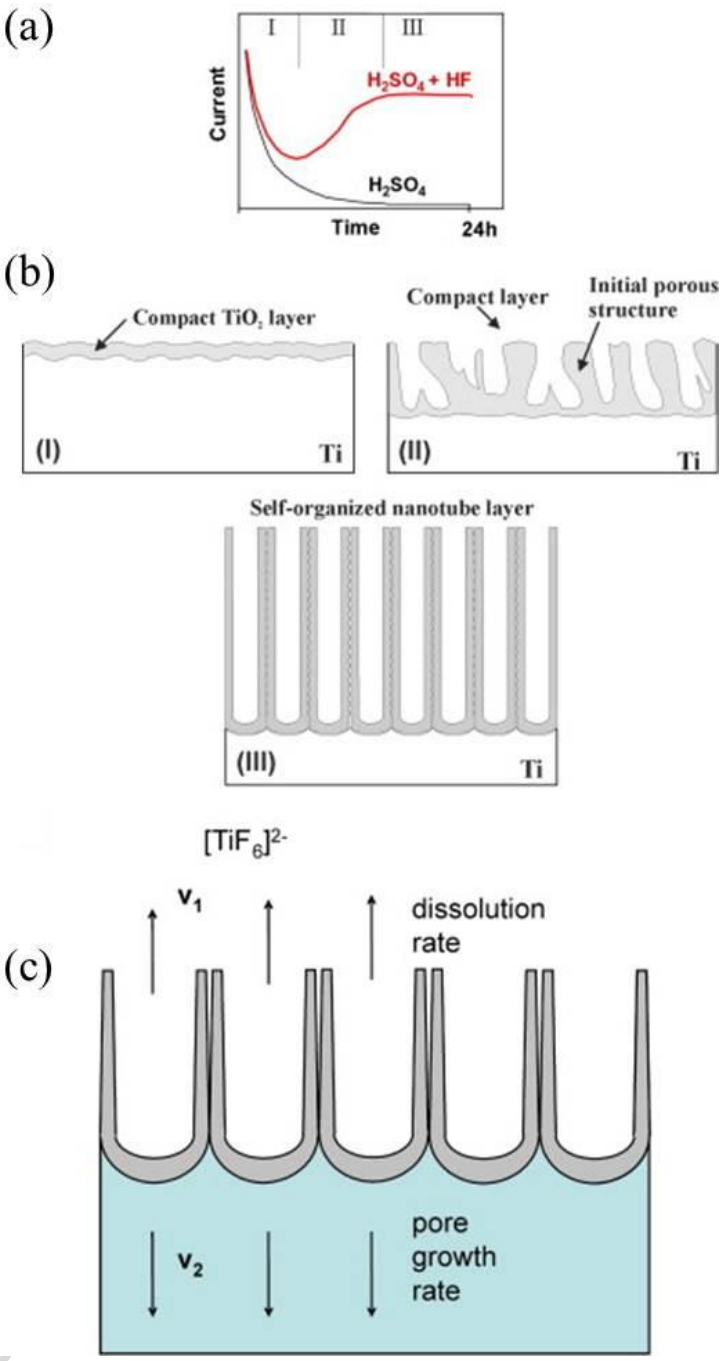

Figure 2 Mechanism of electrochemical anodization of Ti to fabricate titania nanotubes (TNTs). (a) Typical current–time characteristics in fluoride containing electrolytes compared with fluoride-free solution, (b) schematic depiction of the formation of TNTs, and (c) steady state growth stage: TNTs dissolution rate (v_1) = formation rate (v_2). Reproduced with permission from [29], © Elsevier 2007.

2.2 Composition of Anodization Electrolyte

To understand the interface between TNTs and Ti, visualization of the bottom of nanotubes at the point of attachment to the Ti substrate is crucial, which can be obtained by imaging the fractured/peeled-off anodized films (TNTs), easily achievable by mechanical, physical or chemical methods. This closed and domelike bottom of the TNTs is a thin titania layer separating the TNTs from Ti, and is defined as the barrier layer (BL), which commonly existed in nanoporous alumina [32]. Owing to the rounded BL, surface dimples are encountered on the metallic surface, giving it a nano-templated topography. Electrolyte composition, including water content and fluoride concentration, play an important role in controlling the geometrical parameters of the TNTs, including the BL-Ti interface [33].

The water content of the electrolyte (supplying oxygen for the oxidation of Ti) significantly affects both the growth rate and the chemical dissolution speed of TNTs. According to equation (ii); field-enhanced oxidation occurs at the BL-Ti interface, where the oxygen ions (O^{2-}) from the electrolyte combine with Ti^{4+} to form TiO_2 along the direction of the nanotube growth [34]. Valota et al. have shown that the addition of water to fluoride/glycerol electrolytes results in a thicker barrier layer, while also enhancing the expansion factor, which induces the volume difference and stress between the TNTs layer and the Ti substrate [35, 36]. The expansion factor is determined by the volume ratio of oxide to the consumed metal and is called the Pilling–Bedworth ratio (PBR) [37]. Slightly increasing the water content (for systems with water >2%) in organic electrolyte accelerates the dissolution rate of the nanotubes, which in turn can result in decreased nanotube length and increased diameters [38-40]. The most striking characteristic of TNTs formed in aqueous electrolyte is the ripple on the sidewall, and this ring-like structure is occasionally seen in organic electrolytes with low water content (<2.5%) [29, 36]. Occurrence of ripples on the TNT sidewall is the result of competition between the tube growth rate at the bottom and the tube splitting speed at the cell boundaries [41]. Thus, in organic electrolyte systems with limited water content, where the chemical dissolution rate is further decreased by anodization, the nanotubes can be longer and smoother. Furthermore, in long-duration anodization etching of TNT tops becomes apparent, which results in needle-like or grass-like inhomogeneous structures (collapsed and bundled tops), which may compromise the overall stability of the structures. Because this so-called ‘nanograss’ often aggregates during drying to resist capillary actions, it enhances internal stress in the oxide layer and generates an upward force at the nanotube bottom, thereby decreasing the bond strength between TNTs and the metal substrate [42].

As previously mentioned, fluoride ions in the electrolyte strongly influence the anodization process by chemically dissolving TiO_2 and binding ejected Ti^{4+} at the oxide/electrolyte interface. It is noteworthy that as the result of their fast migration rate [33], fluorides accumulate at the nanotube bottoms and cell boundaries in the form of soluble fluoride species (Ti-O-F or Ti-F complexes) to form an additional fluoride-rich interface layer separating the barrier layer and the Ti substrate during the growth phase of TNTs [29], which has been demonstrated by X-ray photoelectron spectroscopy sputter profiles from the bottom side of lifted-off TNTs as seen in Fig. 3(a) [28, 43]. Shimizu et al. demonstrated that the existence of the soluble fluoride-rich layer underneath the nanotube bottoms resulted in poor adhesion of the resultant anodic films [44]. Thus, eventual detachment of the anodic film from the substrate can be observed [45]. After lifting off TNTs, the majority of the remnant flakes of the fluoride-rich layer are visible on the dimples of the Ti substrate, as shown in Fig. 3(b) [28]. Therefore, methods involving an additional fluoride sedimentation procedure in EA [46], or annealing to reduce fluoride content in the overall nanotube layer are aimed at enhancing the adhesion strengths of the TNT films [47]. The fluoride-rich layer is a key reason for the transition of porous structures to nanotubes as the formed layer at the bottom of the nanotubes can move to cell boundaries by a flow mechanism, which is prone to chemical dissolution. This process is schematically depicted in Fig. 3(c) [43].

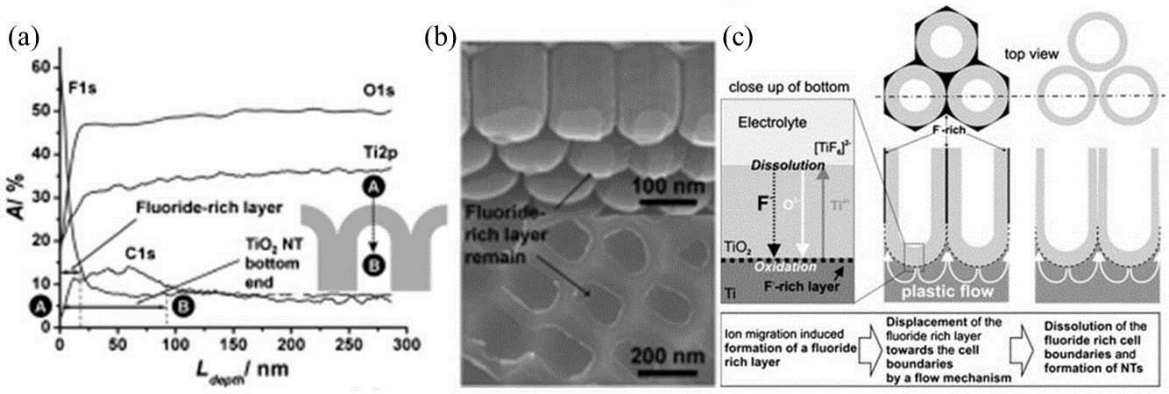

Figure 3 Presence of fluoride-rich barrier layer at the interface of titania nanotubes (TNTs) and the underlying substrate: (a) XPS (X-ray photoelectron spectroscopy) depth profile from the barrier layer of detached TNTs confirming the existence of a fluoride-rich interface layer (reproduced with permission from [28], © WILEY-VCH Verlag GmbH & Co. KGaA, Weinheim 2008), (b) SEM images showing the remaining flakes of fluoride-rich layer both on the bottom of the removed TNTs and at the Ti substrate (reproduced with permission from [28], © WILEY-VCH Verlag GmbH & Co. KGaA, Weinheim 2008). (c) Schematics of

nanotube formation in the presence of fluoride in the electrolyte (reproduced with permission from [43], © Elsevier 2011).

2.3 Aging of Electrolyte

Electrolyte optimization influences the quality and morphology of anodized films, and interestingly aging of organic electrolytes is often used in practice to fabricate highly ordered TNTs, but remains underexplored to date. Aging of electrolyte is the repeated anodization of dummy titanium prior to the fabrication of TNTs on the target substrate. Only a few studies have reported titanium anodization in aged electrolytes, using fluoride containing organic electrolytes with dimethyl sulfoxide (DMSO) [40] and ethylene glycol or glycerol [42, 48-51]. With regard to the effects of previously used electrolyte on TNT dimensions, it has been reported that the previously used DMSO-based electrolyte decreased the length and diameter of TNTs while thickening the tube walls [40]. But in the aged low water content (<2.0%) ethylene glycol based electrolyte, the length, pore diameter and wall thickness of TNTs were higher relative to those in fresh electrolyte, which may be ascribed to the anhydrous nature of ethylene glycol [42]. However, these studies all demonstrated a greatly improved adhesion between TNTs and the underlying Ti substrate. In this section, the effect of electrolyte ageing on the growth rate of TNTs, formation of barrier layer and growth-induced internal stress such as PBR are discussed in detail with focus on the integrity and adherence strength of the TNT film.

It is noteworthy that most studies ignore the hygroscopic nature of the ethylene glycol based electrolyte which may explain the conflicting results obtained with respect to conductivity and growth rates of nanotubes upon ageing of the electrolyte [51]. More recently we have optimized the ageing of the electrolyte in an enclosed electrochemical cell, thereby avoiding any chance of moisture incorporation inside the electrolyte [51]. Repeated anodization or ageing of the electrolyte continuously alters its chemical composition, leading to an increase in $[TiF_6]^{2-}$ content, while the oxygen bearing anionic species are gradually depleted, which further reduces electrolyte conductivity [49]. Meanwhile the formation/dissolution rate of oxide is also hindered [equations (ii) and (iv)], thereby impeding the growth rates of TNT formation [52]. Thus it is reasonable to infer that a thicker oxide BL at the base of nanotubes is formed under these conditions. Comparing with fresh electrolyte, the time to reach the anodization equilibrium phase (with the low and stable value of current density, denoted as t_{eq}) is delayed for aged electrolyte

due to reduced conductivity, which was confirmed by current-time monitoring and electrolyte conductivity measurements [49, 51]. Furthermore, applied anodization voltage is the sum of PD at the metal-oxide interface, across the oxide, oxide-electrolyte interface, and across the electrolyte. Assuming that changes of PD at the interfaces are negligible, PD across the electrolyte increases as the consequence of conductivity reduction, which means a decrease in the PD across the oxide layer [42]. This, in turn, reduces the formation of $[TiF_6]^{2-}$ complexes and hence causes delayed t_{eq}. This can also be linked to the formation of a thicker BL. In these regard, lower growth rates combined with reduced conductivity can result in a thicker compact BL layer representing better contact between the resulting nanotubes and the underlying substrate, and thereby improving the stability of the nanotubes. Changes of electrolyte features and characteristics of as-anodized TNTs in fresh and aged electrolytes are shown in Fig. 4. Furthermore, internal stress develops along with anodic oxidation due to the volume increase of oxide (PBR) [50]. The magnitude of this growth-induced compressive stress depends on the actual fraction of oxide formed at the metal/oxide interface, and the high stress may yield fragile anodic layers [53]. The decreased growth rate of aged electrolyte can reduce the compressive internal stress at the barrier layer-metal substrate interface, thereby yielding stable and well-adherent TNTs. To summarize, with the use of aged electrolyte, a thicker BL with a more compact structure and improved stability can be obtained, leading to an improved stability of TNTs.

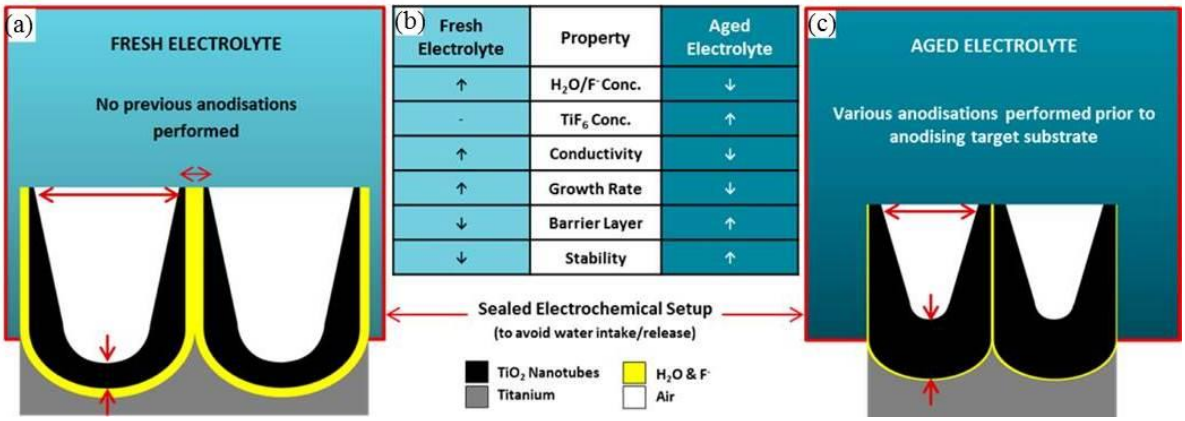

Figure 4 Schematic representation of changes in nanotube and electrolyte characteristics for fresh and aged electrolyte anodization. Reproduced with permission from [51], © American Chemical Society 2015.

2.4 Sterilization without Compromising Stability

Prior to cell studies and implantations *in vivo*, it is crucial to sterilize implants, without compromising the biocompatibility, surface chemistry and mechanical stability. However, studies have suggested that the inconsistent biological performances, especially for the similar range of nanotube dimensions, may be due to varied sterilization procedures utilized, without appropriate investigation of the related changes to the implant surfaces [23]. Furthermore, most studies investigating TNTs modified implant applications, do not detail the sterilization methodology. Recently, few studies have aimed to elucidate the relationship between effective sterilization and biocompatibility [54-56]. Moreover, it is well accepted that any seemingly small change on the surface of implants may influence cellular behaviour, thereby optimizing and investigating the various techniques used for sterilization is crucial. Table 1 summarizes the pros and cons of various sterilization methods with respect to effective cleaning of TNTs-modified implants.

In a pioneering study, Zhao et al. reported that ultraviolent (UV) and ethanol treatment enhanced the wettability of TNTs, compared to autoclaving, whereas UV irradiation induced the best *in vitro* primary rat calvarial osteoblasts responses (owing to effective removal of surface contaminants, especially hydrocarbons) [54]. Later Kummer et al. compared the role of sterilization on bacterial growth on various implant surfaces, including flat Ti and TNTs [55]. Autoclaving resulted in the highest amount of *S. aureus* and *S. epidermidis* growing on implant surfaces compared to UV and ethanol treatment. This was ascribed to the incorporated hydrophobic carbon impurities onto the samples, which may alter surface chemistry and hence bioactivity. Moreover, it was reported that smaller diameter (20 nm) of TNTs and heat treatment induce subtle changes in surface chemistry, roughness, wettability and crystallization, that contribute towards antibacterial efficacy [55]. Furthermore, Oh et al. found that the air entrapment into nanotubes during dry autoclaving dramatically increased the *in vitro* osteogenic functionality of MC3T3-E1 mouse osteoblasts after 24 h incubation [56].

Considering that high temperature and pressure treatments such as autoclaving may compromise the stability of TNTs, more investigations are needed in this regard to ensure the maintenance of nanotube stability. Recently, Junkar et al. reported surface morphology alterations of TNTs sterilized by autoclave, UV irradiation, and H_2O_2/O_2 plasma techniques. Significant changes were observed after autoclaving, whereby TNTs structures (15, 50, 100 nm in diameter) were damaged to some extent at both the top and bottom. Severe destruction was observed on smaller diameter TNTs, where the open mouth of TNT

collapsed while the bottom delaminated. However, the different sterilization methods did not influence the wettability of freshly prepared and sterilized TNTs [57]. Interestingly, in this study only freshly fabricated TNTs were used, as it was reported that ageing turns TNTs more hydrophobic within three weeks [58]. Furthermore, UV sterilization, suggested to be the most favourable sterilization technique, also represents a minimally invasive technique with respect to nanotube stability.

It is worth noting that high temperature/pressure in the presence of moisture, such as inside the steam autoclaving setup, may induce TNTs crystallization [59]. In this context, Yu et al. investigated the mechanism of TiO_2 phase transition by comparing crystallization and morphology changes, using various sterilization treatments including: calcination (annealing at 450°C in air for 3 h), vapor-thermal (autoclaving at 180°C without direct contact of TNTs and water), and hydrothermal (autoclaving at 180°C in wet environment). It was shown that water can act as a phase transformation catalyst to facilitate the crystallization process, which is schematically described in Fig. 5(A) [59]. The water catalysed crystallization reaction tends to first occur at the interface of TNTs and the Ti implant due to the lowest activation energy of interface nucleation [60]. At the same time, titania in the tubular wall remains amorphous, which has higher solubility and surface energy compared to the anatase titania at the bottom. As the hydrothermal time increases, the size of anatase crystallites at the interface grows and amorphous titania are rapidly dissolved, which leads to the eventual destruction of nanotube structures and formation of aggregated anatase nanoparticles [61]. The aforementioned mechanism is further confirmed by the TEM images of TNTs treated by hydrothermal treatment [Fig. 5(B)]. On the contrary, calcination and vapor-thermal treatments induced a different crystallization mechanism without damaging the TNTs. However, slight deformation is occasionally observed at the top of TNTs sterilized by UV irradiation or plasma sputtering, which can etch the TNTs and modify the surface activity [57, 62, 63]. However, their influence on mechanical stability of TNTs is not well understood. Further advancements in this domain can be realised by varying the experimental parameters such as the wavelength, irradiation time, and intensity for UV treatment, and pressure, gas composition and flow rate for plasma treatment, which needs to be optimized for improved and reproducible outcomes.

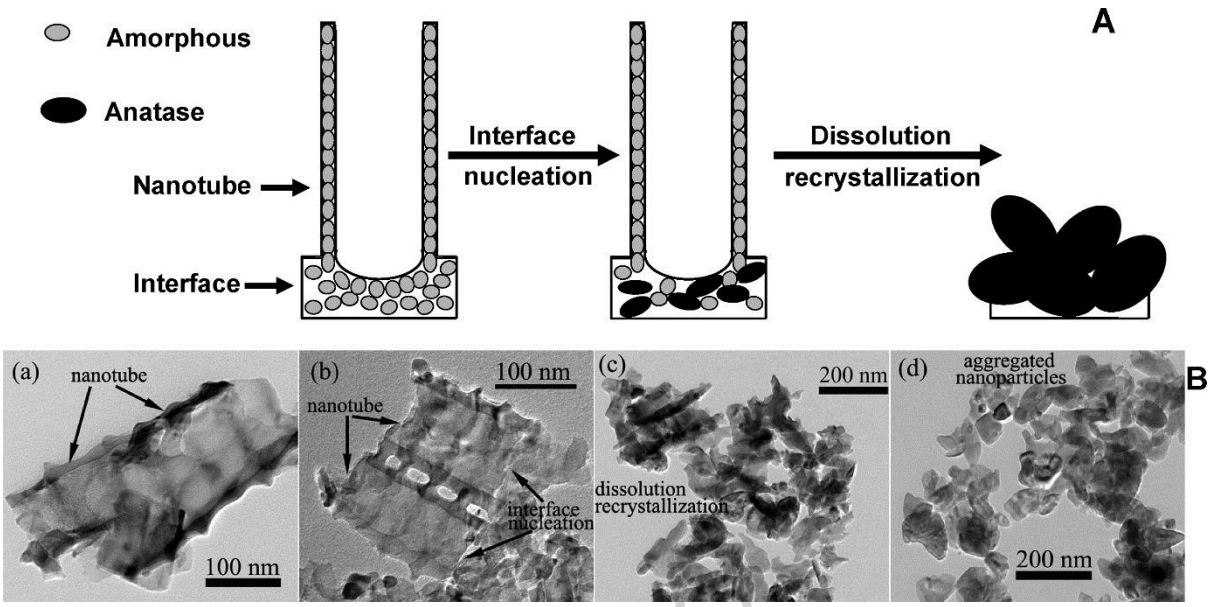

Figure 5 Effect of autoclaving on crystallization of nanotubes: (A) scheme showing transformation of amorphous nanotubes to anatase, and (B) TEM images showing the morphology evolution of TNTs hydrothermally treated at 180 °C for (a) 0 min, (b) 15 min, (c) 30 min, and (d) 2 h. Reproduced with permission from [59], © American Chemical Society 2010.

Table 1 Methodology and research gaps of commonly used sterilization methods for titania nanotube (TNT) modified implants.

Sterilization Technique	Methodology	Research gaps	Ref
Autoclaving	High temperature/pressure treatment, in presence of adequate moisture (wet) or in the absence of moisture (dry)	• Deposition of hydrophobic contaminants • Destruction of TNTs by wet autoclaving • Effects of air entrapment in dry autoclaving	[56, 57, 64]
Ethanol Immersion	Immersion in absolute or 70% ethanol	• Potential contamination (if ethanol is not removed) • Compromising stability of TNTs upon quick drying	[54, 55]
UV Irradiation	UV induced sterilization based on decomposing contaminants, which may be enhanced by photocatalytic activity of TiO_2.	Parameters unexplored: amplitude, wavelength, irradiation time, intensity	[54, 65]
Plasma Treatment	Sputtering plasma to decontaminate	Precise optimization of plasma conditions (pressure, gas composition and flow rate etc.)	[62, 63]

2.5 Influence of Underlying Titanium Substrate Topography

The geometry, topography and chemistry of the target Ti metal substrate can influence the characteristics, including the mechanical stability of the fabricated TNTs film [51]. For instance, Ti surface pretreatments (polishing/pre-anodizing in fluoride-free electrolyte) have been utilized to alter the formation of nanotubular or nanoporous morphologies, whereby in such systems, fabrication of nanopores is favored on the polished Ti surfaces [66]. With progress in EA techniques, it has been recognized that polished Ti substrates yield an improved alignment of TNTs with reduced surface defects (weak spots or poor mechanical stability) [67]. To address this, various surface smoothening treatments including mechanical, chemical and electro-polishing have been applied to reduce Ti substrate roughness, and the resultant effect on the growth/morphology of TNTs has been investigated [68]. As reported by Smith et al., chemical polishing (immersion in $HF/HNO_3/H_2O$ mixture) smoothened the surface, however resulted in unavoidable micro-scale defects [69]. Both mechanical polishing (grinding by abrasive papers) and electro-polishing (anodizing in perchloric acid electrolyte) of Ti resulted in a desirable smoothness for anodization, while the electro-polished sample had the lowest roughness [68, 70].

Furthermore, chemical pitting by F^- from the electrolyte takes place at the oxide layer, which is formed at the very beginning of the EA process. This F^- attack is most prone to occur at the defect sites because of the relative higher electrolyte distribution. By the direction of pitting holes, nanopores are generated unevenly on the rough as-received surfaces, which are followed by self-ordering of nanotubes underneath, and meanwhile, the porous layer is gradually dissolved [71]. By contrast, on the as-polished surfaces the nanopores are formed randomly and retained. As described by Shin et al., the electro-polished smooth Ti surface was beneficial to the formation of a thin and uniform nanoporous layer, and highly ordered TNTs [72]. For mechanically polished Ti, Xing at al. found that the upper nanopores on the polished surface were rough and mainly aligned along the scratch lines [70]. The nanoporous top layer has relatively low solubility due to the contained anatase or rutile titania, which effectively acts as etching protection for the underlying nanotubes [66, 71]. In the absence of this porous layer, chemical dissolution takes place at the nanotube mouth leading to the formation of the disordered “nanograss” structure as the reaction time continues, which is mechanically unstable when removed out of the electrolyte, often leading to the tubes clumped as bundles (compromised stability) [73]. When these two structures are subjected to external compression forces (nanoindentation), the nanopores are more stable than nanotubes, as they are connected

with the surrounding pores, which enables sharing/distribution of the applied force, while the individual nanotubes are successively fractured due to the absence of mechanical interactions [74]. Interestingly, these more mechanically robust nanoporous structures have not as yet been applied towards enhancing the bioactivity of Ti based implants.

With the progress in EA, a more commonly used two-step anodization approach was developed for fabricating highly ordered TNTs arrays [75]. The first-step anodization provides well-ordered hexagonal imprints by removing the as-formed TNTs, which serve as the template for the growth of TNTs in the second-step in order to generate hierarchical top-porous/bottom-tubular titania nanostructures [70]. The novel two-step Ti anodization notably outperformed the conventional one-step anodization due to the greatly improved size uniformity and alignment of TNTs, which has been reported to have enhanced photo-electrochemical properties, while being rarely investigated in the biomaterial domain [76, 77]. The two-step anodized TNTs are closely packed with surrounding tubes and covered with a smooth nanopore array, and as a result the mechanical stability may be improved. Besides, repeated anodizations of a Ti substrate may totally eliminate the need to perform surface smoothening in the first place, however this hypothesis remains unexplored.

3. Strategies to Augment Mechanical Stability of TNTs

Long-term mechanical stability of the biomaterial coating is crucial for the life-long success of bone/dental implants. Mechanical properties, including hardness, elastic behaviour and adherence strength, are particularly important and must be investigated for all implant surface modifications. Implant coating delamination/deformation may occur during surgical placement or upon post-implantation loading. Indeed, following implantation, material destruction or bone resorption may take place when there is a mismatch in the mechanical properties of the bone and the implant. For instance, the elastic modulus of human cortical and trabecular lamellar bone is 13.5-25.8GPa, which is above many of the reported modulus values of commonly used biomaterials and their surface modifications [78]. Notably, as-anodized TNTs can easily be peeled off by mechanical bending [31, 94], and hence it is crucial to augment their mechanical properties. Table 2 summarizes the modified anodization conditions and physical/chemical treatments post-fabrication utilized to augment the mechanical stability of TNTs, and these will be examined in detail in the remainder of the review. Furthermore, the mechanical stability of the TNTs can be assessed using a variety of methods, and these are also outlined in Table 2. Among these, the nano-

indentation technique is appropriate for testing mechanical properties, including the elastic modulus and hardness of TNTs modified Ti implants, due to the low load (1mN) and small displacement (1nm) employed in this method [79]. In addition, axial fatigue, tensile, scratch and wear testing are also utilized to measure the adhesion strength of TNTs to the substrate [31, 46, 84, 85, 87, 88, 95, 96].

Table 2 Overview of techniques used to enhance the mechanical stability of titania nanotubes (TNTs). (EG: ethylene glycol)

Treatment Type	Treatment Methodology [Anodization Electrolyte]	Mechanical Testing	Findings	Ref.
Standard Anodization	20 V/15min, 2h [1M H_2SO_4+0.1M NaF+0.2M citric acid]	Nano-indentation	Young's modulus of TNTs was 36–43 GPa. Thinner films (L_{15min}=230-250nm) had higher values but delaminated.	[80]
	20 V/15min, 4h [1M H_2SO_4+0.1M NaF+0.2M citric acid]	Nano-indentation, interfacial force microscopy	Young's modulus of TNTs was around 4 -8 GPa, with minimal effect from Ti substrate.	[81]
	30V/30, 60, 120, 240min [Glycerol+0.5%NH_4]	Tensile pull-off adhesion strength	Adhesion strength of TNTs < 4.5MPa. Electrolyte agitation contributed to poor adhesion.	[31]
	5,10,15V/180min, 20V/200min [H_2SO_4+0.15%HF]	Nano-indentation	Fracture strength for TNTs (55–110 nm diameter) was around 3 GPa, and 5GPa for 30 nm diameter.	[74]
	30V/48h [Glycerol+0.25%NH_4F+20% water]	*In situ* TEM, nano-indentation	Young's modulus values of individual TNTs (8-10 μm length) was 2.2–9.4 GPa, thinner films had higher values.	[82]
	60V/48h, [EG+0.25%NH_4F+2% water]	Nano-indentation, SEM	Young's modulus and hardness of TNTs were 5.1 GPa and 93.8 MPa. Deformation of TNTs occurred via densification and discrete brittle fracture.	[83]
	20V/1h, without stirring [$(NH_4)_2SO_4$+0.5%NH_4F]	Axial fatigue test, SEM	Ti alloys' fatigue response unaffected by anodization. TNTs remain crack-free after testing.	[84]
Altered Anodization	58 V/15min, 17h, 17h aged electrolyte [EG+0.3%NH_4F+1.0–12.0 % water]	SEM	Moderate water content (3%) and previously used electrolyte can improve adhesion/stability between TNTs and the Ti substrate.	[42]

	60-120V/10-180 min, aged (fresh to >30h) electrolyte [EG+0.3%NH_4F+1.0–3.0 % water]	SEM	Aging of electrolyte (~10 h) led to better stability of the TNTs film. 1% water at 75V/10−40min generated well-adherent and mechanically robust TNT films.	[51]
	1st Anodization step in NANOTI AN I Electrolyte, at 20V/180 s, and 2nd Anodization step NANOTIAN II at 15V/60s.(NANOTI Ltd., UK)	Scratch resistance test , screw test (solid rigid polyurethane foam blocks)	2-step anodization grew nano-pitted anodic films to improve mechanical integrity and tensile strength compared with nanotubular films (anodized in 0.6 wt% NH_4F +3 wt% H_2O+$C_2H_4(OH)_2$ at 80V/15min).	[85]
Anodization of Coated or Modified Titanium	Ti sputtered Alumina plate was anodized at 20V/75min, annealed at 450 °C and 650 °C in N_2 atmosphere. [EG+0.5%NH_4F+25% water]	Nano-indentation	Young's modulus (42.8~117.5 GPa) and hardness (1.9~2.8 GPa) of TNTs increased with annealing temperature.	[86]
	Sputter deposition of Ti on stainless steel 304 substrates, anodized at 25V/60min, annealed at 280 °C, 430 °C and 620 °C in N_2 furnace. [EG+0.5%NH_4F+25% water]	Nano-indentation, micro-scratch test	Young's modulus (55.1~138.42 GPa), hardness (1.753~3.426 GPa) and adhesion strength of TNTs increased with annealing temperature due to the phase transformation.	[87]
	Segmented polyurethane coated on Ti, anodized at 20V/20-300min. [H_3PO_4+0.5%NaF]	Tensile test	TNTs attained higher adhesive strength (~20Mpa) when anodized for <60min.	[88]
Physical Modification and Annealing	Anodizing at 60V/40h, and annealing at 450°C/3h [Dimethyl sulfoxide +2%HF].	Direct force measurements (AFM TEM holder equipped with a MEMS force sensor)	Young's modulus was 23 GPa and 44 GPa for thin-wall (external diameters of ~75, internal diameters of ~65nm) and thick-wall TNTs (external diameters of ~110 nm, internal diameters of ~80 nm).	[89]

	Anodizing at 30V/90min, and annealing at 300, 440, 500°C/2h. [Glycerol+0.25%NH_4F+20% water]	Nano-indentation，Vickers hardness test	Phase transformation of TNTs yields enhanced Young's modulus and hardness.	[90]
	Anodizing at 30V/2h, and annealing at 500°C/5 h and 10 h. [Glycerol+0.5%NH_4F+20% water]	Rockwell C indentation (according to the VDI 3198 standard), EDS, XPS	More Ti-O bonds were formed in the oxide/metal interface with increasing annealing time, improving adhesion of the TNT layers. Thinner TNT film presented better adhesion quality.	[91]
	Anodizing at 20V/1h, and annealing at 325, 450, 600°C/2h. [Citric acid+0.5%NaF]	Nano-indentation	TNTs transformed from amorphous to anatase/rutile with increased annealing temperature, improving Young's modulus and hardness.	[92]
	Nb sputtered Ti67 alloy was anodized at 20V/240min, and annealing at 440°C/30min. ［EG+0.5%NH_4F+5%H_2O]	Vickers hardness, wear test	Mixed oxide nanotubes (TiO_2–Nb_2O_5–Al_2O_3) were fabricated by a multi-objective PSO algorithm optimized anodizing technique, and showed superior hardness and tribological features	[93]
	Laser micro-patterned titanium, anodized at 60V/2h. [EG+0.5%NH_4F+5% HF]	Chemical peel-off test ($HgCl_2$, HCl)	Micro-patterning required longer reaction time and higher chemical concentration to peel-off TNTs. Enhanced mechanical adhesion between TNTs and substrates and long-term stability.	[94]
Chemical Modification	Anodizing at 20V/2h, annealing at 450°C/2h, and thermal treatment in acetylene at 900°C/10min. [Glycerol+0.27M NH_4F+50% water]	Nano-indentation, shear Tensile, friction test	TNTs became semi-metallic via incorporation of Carbon. Hardness, tensile strength and friction behavior improved.	[95]
	2nd stage anodization with addition of magnesium acetate (0.04, 0.048, 0.06, 0.072, 0.088, 0.1 and 0.16 M) at 60-140V/60 min and 80V/30-120min. [EG+0.08M NH_4F+2%H_2O]	Scratch test	Critical load (indicating adhesion strength of TNTs) increased from 3.2N to 17.5N for 0.06 M Mg^{2+} at 80V/70min.	[46]

	HA electrodeposited on anodized (20V/45min) TNTs. Annealing at 450°C, 600°C/30min in argon gas. [0.5M H_3PO_4+0.12M NaF at 20V/0.5h]	Tensile test	Heat treatment improved bond strength of HA electrodeposited TNTs from 16-21MPa to around 44MPa with temperature increase.	[96]
Deposition on Fabricated Nanotubes	Coating TNT films with Al_2O_3 layers (1, 10 and 42 nm) by atomic layer deposition, annealing at 870°C/1 h. [15h aged EG 0.176M NH_4F+1.5%H_2O at 60V/4h]	Nano-indentation	Annealing and Al_2O_3 layers enhanced the mechanical properties of TNTs. Increased hardness occurred with increasing thickness of the Al_2O_3 layers.	[97]

3.1 Modified Anodization Parameters

In a pioneering study, Crawford et al. [80] investigated the mechanical behaviour of TNTs using the nano-indentation technique and reported that the elastic modulus (E) of TNTs was in the range of 36–43 GPa, which was similar to another study conducted by Shokuhfar et al. (23-44 GPa) [89]. However, the nanotubes became densified under the indenter during loading, and the measured E values were actually higher than the intrinsic value of the porous TNT film [80, 83]. Thus, researchers used the nano-indentation technique equipped with *in situ* transmission electron microscope (TEM) and interfacial force microscopy (IFM) to precisely control the indentor displacement, and reported much lower E values (2.2–9.4 GPa) of the individual TNT [81, 82]. The elastic behaviour is also dependant on the nanotube geometry/dimensions: TNTs with smaller length and thicker walls tend to get higher E values [74, 82, 89]. In contrast, hardness varies greatly in the range from 93.8MPa [83] to 3.5GPa [95, 98, 99] for different titania-based nanostructured materials. In the case of TNT films and their adhesive strength, the hardness has been reported to be less than 4.5MPa [31], which is less than the stipulated criterion of at least 18MPa for biomaterial coatings [96]. However, Hieda et al. reported a higher adhesive strength (20MPa) by limiting the anodization time to 1h. A longer anodization time has been postulated to decrease the strength by dissolving the nanotube walls [88]. However, the fabrication conditions of the tested TNTs varies in terms of anodization electrolyte and parameters (time/voltage), and hence the mechanical properties cannot be directly compared (Table 2). Zhu et al [42] and Gulati et al [51] undertook systematic investigations on the optimization of anodization parameters especially by controlling the water content and the age of electrolyte, respectively. Mechanically stable and firmly adherent TNTs were obtained both on flat and curved Ti surfaces by anodizing in low water content (1%-3%) and appropriately aged organic electrolytes (see section 2.3). More recently, a novel nano-pitted (NP) titania structure was proposed by Weszl et al. for improving the mechanical integrity and corrosion resistance over the conventional nanotubular structure, which occurs possibly due to less fluorine dopants in NP anodic film [85]. Moreover, sputtering Ti on other commonly utilized materials, for instance alumina and stainless steel 304, and anodizing the sputtered layer is considered to be a promising approach for increasing the corrosion and wear resistance of the virgin materials, while enhancing the elasticity, stiffness and adhesive strength of TNTs [86, 87].

3.2 Physical Treatment

It is well accepted that the as-prepared amorphous titania crystallize into anatase when the annealing temperature is increased to above 280°C and further transfer to a rutile phase at 500-600°C. During crystallization, the TiO_6 octahedra are rearranged, yielding an improved mechanically stable structure without influencing the structural morphology [59]. Titania in the rutile phase is more mechanically robust than anatase, as its octahedra shares four edges instead of four corners in the anatase octahedra [97]. Hence, there is increasing interest in annealing the amorphous TNTs in order to enhance the elastic modulus, hardness and adhesive strength [89-93]. In a pioneering study, Wang et al. reported significantly enhanced stability of micro-patterned TNTs, which were fabricated by laser micro-machining the Ti surface followed by EA [94]. The laser pre-treatment enhanced the TNT adhesive strength to the substrate during external solvent attack, a finding that was ascribed to the expanded interfacial area [94].

In addition, the deposition of an appropriate secondary material on the fabricated TNTs is another treatment aimed at improving the mechanical properties. Kar et al. coated TNTs with hydroxyapatite in order to enhance the bond strength, and subsequent annealing further improved this strength due to the improved crystallization of hydroxyapatite and inner diffusion of Ca and Ti ions at the oxide/metal interface [96]. Furthermore, pulsed electrodeposition allowed for a firm vertical growth of hydroxyapatite crystals inside the TNTs from the bottom to the top surface at low temperature. In a similar study, Zazpe et al. reported a substantial enhancement of hardness of the TNT layers by depositing Al_2O_3. The heat treated Al_2O_3-coated TNTs exhibited higher hardness with increasing coating thickness, which was attributed to more Al_2O_3 mass within the TNTs and increased content of rutile titania [97]. Undoubtedly, some of these modifications may alter the surface chemistry of the nano-engineered implant and thereby can influence cellular interactions, which is an issue that requires further exploration.

3.3 Chemical Modification

It is reported that the incorporated carbon in TNTs can act as a crystal phase transition inhibitor [100]. In this context, Patrik et al. reported significantly enhanced mechanical properties of carbo-thermally treated TNTs [95]. By converting conventional TNTs to semi-metallic oxycarbides (TiOxCy) and TiC, the increased number of carbide species yielded an overall enhanced mechanical stability of the TNT films. For instance, the

increased hardness of the TNTs was macroscopically identifiable when bending TNTs-Ti samples at 180°. The untreated TNTs showed a considerable number of cracks and even partial delamination near the bending line, whereas only a few isolated cracks were detected on the carbonized TNTs. The hardness value was further quantitatively analysed, and was shown to be greatly improved from 0.5GPa at 300°C to 2.5 GPa at 800°C (in the presence of acetylene). Furthermore, the tensile strength and friction behaviour were also improved by the thermal carbonization [95]. Importantly, apart from the enhanced wearability, TiC and its sub-oxides are also reported to be biocompatible [101].

Zhang et al. reported an alternative modified anodization protocol involving the sedimentation of F^- ions in the fluoride-rich layer by adding magnesium acetate at the later stage of the standard anodization process [46]. The resultant TNTs presented a compact fluoride-free amorphous titania layer at the interface of the nanotube bottoms and the Ti substrate without compromising the surface morphology. However, other parameters such as sedimentation voltage/time and $(CH_3COO)_2Mg$ concentration can also influence the adhesion strength. Thus, a broad range of experiments were performed in this study to explore the most optimized parameters for the sedimentation process, including voltage (60-140 V), time (30-120 min) and Mg^{2+} concentration (0.04-0.16 M). Finally, the optimized process yielding the most significant improvement in the adhesion strength of TNT arrays was identified as standard anodization performed at 60V for 60min (electrolyte: EG + 2% H_2O + 0.08 M NH_4F) followed by an additional anodization at 80V for 70min by the addition of 0.06 M Mg^{2+} to the former electrolyte [46].

4. TNTs Stability inside the Bone Micro-Environment

In addition to the considerable volume of literature that has reported on the laboratory testing of key mechanical properties of TNTs, several *ex vivo* and *in vivo* studies have also been conducted to investigate the ability of TNTs to withstand the forces experienced upon insertion into bone, as well as following post-implantation loading (Table 3).

Table 3 Overview of mechanical testing of titania nanotubes (TNTs) post-implantation in animal tissues *ex vivo* and *in vivo*. (EG: ethylene glycol)

Implant Placement	Anodization Conditions	Nanotube Dimensions	Treatment Post Fabrication	Implantation	Mechanical Test and Findings Post Implant Retrieval	Ref.
Ex vivo	(i) 1% HF in DI water, at 20 V/45 min, (ii) EG [1% HF, 0.5% NH_4F, 10% water], at 40V/1h.	L_i = 300 nm L_{ii}= 950 nm D = 100 nm	Electrodeposition of nano-particulate Ag	Equine cadaver bone *ex vivo* (14 days)	SEM imaging: no significant delamination/damage for TNTs. Ag-TNTs did not compromise adhesion to Ti.	[102]
	EG [2.5% water, 0.1M NH_4F] with 1.5 M lactic acid, at 60V/20min.	L = 17 µm D = 70 nm	Loading of Rhodamine B via immersion	Bovine trabecular bone cores *ex vivo* using ZetOS bioreactor (11 days)	SEM imaging: no delamination/damage.	[104]
	EG [1.0% water, 0.3% NH_4F], at 75V/120min.	L = 32 µm D = 90 nm	Loading of parathyroid hormone via immersion	Bovine trabecular bone cores *ex vivo* using ZetOS bioreactor (5 days)	SEM imaging: TNTs retained integrity without deformities/delamination.	[105]
	EG [1.0% water, 0.3% NH_4F], 75V/120min.	L = 9 µm D = 50 nm	TRAIL (TNF-related apoptosis-inducing ligand) loaded TNTs	3D matrigel plug *ex vivo* (24h)	SEM imaging: TNTs arrays presented no loss of surface integrity during 3D culture with matrigel.	[107]
In vivo	H_3PO_4 with 0.3% HF, at 5 V/1 h.	L = 100 nm D = 30 nm	Sterilized using γ-radiation	Frontal skull of domestic pigs *in vivo* (90 days)	SEM imaging: Shearing forces during implantation did not damage TNTs integrity	[108]
	EG [1.0% water] with 0.3% NH_4F, at 75V/120min.	L = 9 µm D = 50 nm	TRAIL loaded TNTs for anti-cancer therapy *in vivo*	Subcutaneous tumor of nude BALB/C mice *in vivo* (6 days)	SEM imaging: TNTs were intact after removal from tumor.	[107]
	0.3% HF aqueous electrolyte, at 20V/30min.	L = 250 nm D = 100 nm	Annealing at ~550°C and autoclaving for 121°C for 30 min	Rabbit tibia *in vivo* (4 weeks)	Tensile testing: Interface of TNTs to Ti was not fractured by pull-out force.	[109]
	Commercial self-drilling anodic oxide Ti miniscrew (1.5 mm diameter; 7 mm length)	–	–	Mandible of beagle dogs with an immediately applied orthodontic force of 250g after insertion for 12 weeks (*in vivo*).	SEM and AFM imaging: Surface of the retrieved anodic oxidized mini-screws in the thread edges were changed by self-drilling insertion and initial loading, especially in the screw tip area.	[110]
	2nd anodization in EG with 0.5% NH_4F, at 60V/15min.	L = 5 µm D = 110 nm	–	Legs of New Zealand white rabbits *in vivo* (8 weeks)	Focused ion beam: TNTs on thread edges were damaged due to self-drilling, others were well maintained.	[111]

4.1 *Ex Vivo* Implantation

To study the insertion and survival of TNTs in bone, Shivaram et al. conducted a mechanical *in vivo* stability study using TNTs (lengths 300 and 950 nm) on Ti rods with/without silver deposition, by implanting into equine cadaver bone *ex vivo* [102]. The implantation procedure consisted of drilling a hole in the bone, followed by a hammered insertion process mimicking the clinical surgical procedure. The Ti rods were retrieved 14 days later and observed under SEM. Both sets of TNTs (with/without silver) showed no sign of macroscopic damage or delamination. Furthermore, the implantation did not impact on the release profile of the antibacterial Ag ions from Ag-TNTs. The presented release profiles suggested that Ag was released in a sustained fashion below the toxic limit, and additional human fetal osteoblast culturing showed no cytotoxic effect from the use of Ag-TNTs.

It is worth noting that the bone recipient site post implant placement represents a complex micro-environment with a variety of interactions between different cell types, interstitial fluid, various serum proteins and the implant material itself which may influence the therapeutic effects of TNTs as well as their mechanical behaviour [103]. Thus a three-dimensional (3D) bone reactor-Zetos^{TM} system has been developed to explore the drug release and stability of nano-engineered Ti implants in bone *ex-vivo* [104, 105]. The Zetos^{TM} bone bioreactor not only maintains bone viability for at least 3 weeks by continuously perfusing culture medium but can also exert physiologically relevant cyclic loading to evaluate the mechanical behaviour of the cultured samples (the latter remains unexplored for TNTs based implants) [106]. Rahman et al. used Rhodamine B (RhB) as a fluorescent model drug to load into the TNTs/Ti wires (fabricated in lactic acid-ethylene glycol electrolyte). RhB loaded implants were manually inserted into the trabecular bone cores with previously drilled holes and cultured for 11 days using the Zetos^{TM} system with different bone micro-environments (with marrow removed, marrow intact and marrow + anticoagulant heparin). It was confirmed that the release profiles varied under different conditions, and the attachment between the bone core and TNTs was improved in the presence of marrow. However, the retrieved TNTs all retained their integrity without any observed deformation or delamination (Fig. 6) [104]. The mechanical stability of TNTs inside bone *ex vivo* using Zetos^{TM} was also demonstrated by Gulati et al, where TNTs/Ti wires (conventional ethylene glycol electrolyte) with surface cracks (diameter 90 nm and length 32µm) were inserted into bovine trabecular bone cores *ex vivo*, and then cultured for 5 days [105]. The examination of TNTs post retrieval confirmed the stability of the

nanotubes. Thus the Zetos^{TM} bone bioreactor appears to be a promising way to bridge the gap between the *in vitro* and *in vivo* settings. In addition, Kaur et al. established a 3D cell culture method using a matrigel plug *ex vivo,* and demonstrated a significant anticancer effect of drug-loaded TNTs-Ti wires, while maintaining their surface integrity [107].

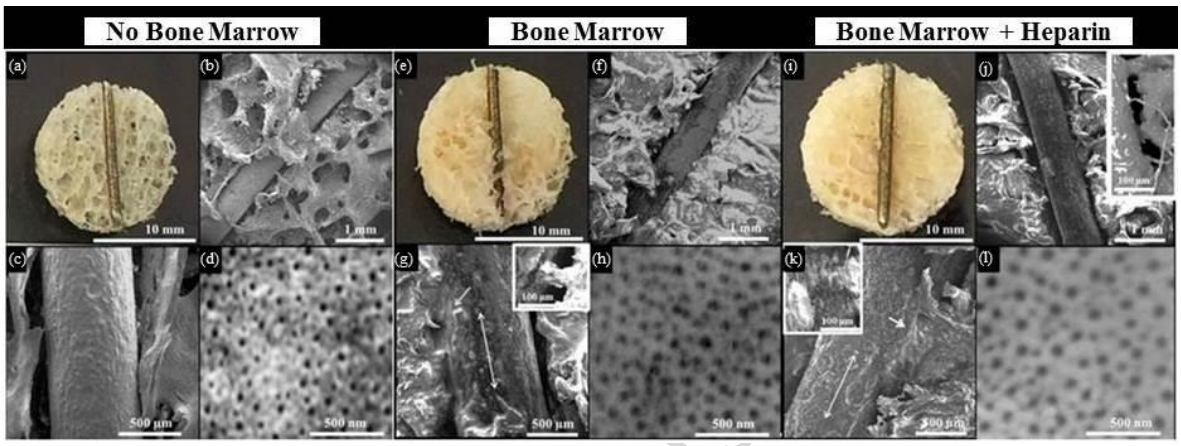

Figure 6 Integration and mechanical stability of drug-loaded TNTs/Ti wire implants in various trabecular bone environments *ex vivo:* (a,e,i) cross-section photograph of implant inside bone core, (b,f,j) SEM images of implant inside the bone, (c,g,k) high-magnification SEM image indicating extent of integration, (d,h,i) top-view of the TNTs with intact morphology. Arrows indicate integration/attachment between the implant surface and bone core. Reproduced with permission from [104], © Wiley Periodicals, Inc 2015.

4.2 *In Vivo* Implantation

For easy translation of TNT implant technology to clinical applications, thorough *in vivo* testing is necessary to ensure the stability of the nanotubular structure in a load bearing dental/orthopaedic implant setting. In a pioneering study, von Wilmowsky et al. inserted anodized Ti rods into the frontal skull of domestic pigs *in vivo* and upon retrieval found that the nanotubes were intact on Ti implants for up to 90 days [108]. Pull-out testing was also utilized by Bjursten et al. to investigate the bond strength between rabbit tibia and Ti implants with heat-treated TNTs *in vivo,* compared with grit-blasted surfaces [109]. The results confirmed that the bonding strength was improved by approximately 9-fold, and a fracture force of up to 10.8N was inadequate to compromise the adhesion strength between TNTs and Ti [109]. Ensuring the translation into dental implant market, screw shaped Ti implants were also used to evaluate the structural stability of TNT modifications during

self-drilling implantation and constant load-bearing conditions in the mandible of beagle dogs *in vivo* [110]. The smoothed thread edges (as measured by AFM) implied that TNTs may have been damaged either by the insertion shearing force or orthodontic tension. Obvious surface change was found at thread edge close to the tip as shown in Fig. 7, whereas deformation of the TNT arrays on the middle or bottom thread edges could not be confirmed by SEM images. Furthermore, two-step anodized TNTs on the mini-screws were also unavoidably damaged at the thread edges during the self-drilling process [111]. More recently, the mechanical stability of TNTs was also investigated in a cancer therapy model by Kaur et al [107]. Briefly, TNTs modified Ti wires as carriers of an anti-cancer agent (TNF-related apoptosis-inducing ligand: TRAIL) were inserted into mice tumour sites *in vivo* and were retrieved after 6 days. The TNTs demonstrated effective local anti-cancer therapy and successfully maintained their structural integrity [107].

To summarize, the available literature provides some proof of the mechanical stability of TNT/Ti based bone/dental implants, but there has been limited emphasis on investigating the Ti screws design or quantitative analysis of mechanical properties in the *in vivo* setting. Such implants are expected to perform in more challenging situations, such as functional mastication and orthopaedic loading environments (joint replacements and fracture corrections) in the presence of physiological fluids, and hence long-term *in vivo* testing in clinically relevant conditions are needed to bridge the gap between the laboratory and the clinic, towards designing the next generation of orthopaedic/dental implants.

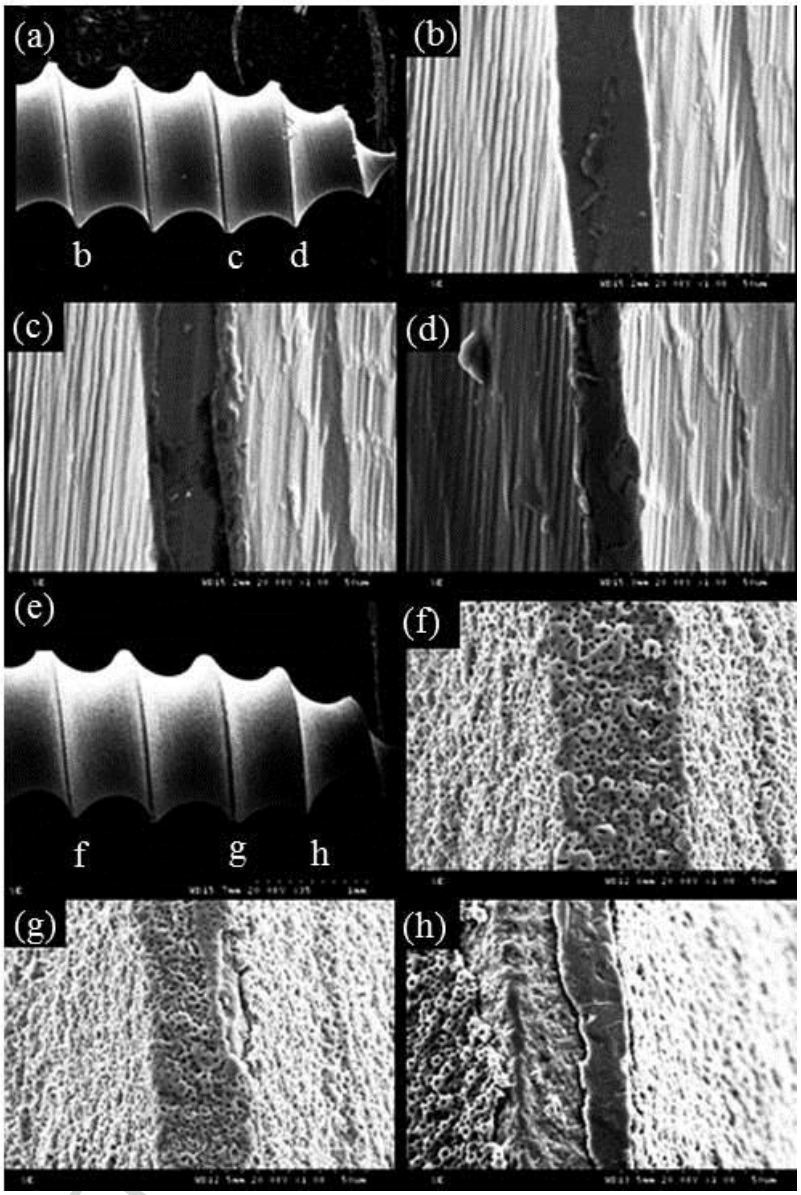

Figure 7. SEM images of retrieved Ti mini-screws from the dog mandible *in vivo*: (a) machined mini-screw as control; (b) thread edge at the bottom; (c) thread edge in the middle of the screw; (d) thread edge at the tip area; (e) anodized mini-screw; (f) thread edge at the bottom with tubulure structures; (g) thread edge in the middle of the screw, TNTs undamaged; (h) thread edge close to the tip of the anodized mini-screw, TNTs were destroyed by self-drilling insertion and initial loading. Reproduced with permission from [110], © The E. H. Angle Education and Research Foundation 2017.

5. Conclusions and future perspectives

This review highlights the progress made in the domain of anodized titanium with titania nanotubes (TNTs) with enhanced mechanical performance to ensure long-term success in load bearing conditions, such as orthopaedic and dental implants, without the risk of mechanical failure. With the advancements in electrochemical anodization (EA), the fabrication of self-ordered TiO_2 nanotubes/nanopores on the surface of titanium, lead to the popularity of these nanostructures with applications ranging from bioactive/drug-releasing implants to solar cells and catalysis. While most research encompassing TNTs focused on enhancing their applicability, an important criteria was often ignored. The sub-optimal mechanical stability of these structures could compromise the long-term functioning of these devices. Focused on orthopaedic and dental, this review discussed the need for stable nanotube coatings on titanium implant surfaces, which could survive the mechanical handling, implant placement surgery and the long-term survival in a constant load bearing bone/dental micro-environment.

Towards optimizing the fabrication of TNTs, an understanding of the interface between TNTs and Ti is crucial. While numerous parameters needs to be tuned, we discussed the influence of electrolyte composition and electrolyte ageing, which are inter-related but remains underexplored. The concentration of water and fluoride ions in the electrolyte is vital towards deciding the growth rate and the formation of nanopores or nanotubes. In fact the repeated use of electrolyte to 'prepare' or 'age' the electrolyte, prior to anodizing target substrate, has shown promising outcomes with respect to achieving mechanically stable nanotubes, especially on the complex geometry of Ti implants. It is worth noting that with a handful of research reporting the influence of ageing the electrolyte, this field still remains underdeveloped. The balance between TiF complexes (increased) and water content (reduced) during this ageing in a moisture-controlled system, results in a highly optimized electrochemical system, with the resultant nanotubes formed with a thicker barrier layer, with relatively reduced growth rate, but with significantly enhanced mechanical properties.

It has also been suggested that the discrepancies with respect to varied cellular functions for a similar range of TNTs may be due to the varied sterilization techniques used. Again representing a research gap, most publications use different strategies: ethanol, UV, autoclave and plasma. Among these, not only is the UV irradiation is the safest in terms of not compromising the stability of the nanotubes, but also enhanced the bone cell activity. Clearly the use of high temperature/pressure systems (autoclave) or use of liquids

(water/ethanol) may change the surface chemistry (contaminants) and the drying of the liquids may induce surface instabilities leading to defects/breakage.

With respect to substrate preparation, a more commonly practised strategy is to polish titanium to remove surface defects, resulting in a smooth finish ready for anodization, which yields improved nanotube ordering and reduced defects. Such substrate pre-treatment can be performed via mechanical, chemical or electro-polishing, which in turn can dictate the formation of pores or tubes. Besides, removing the anodized layer prior to re-anodizing (2-step EA) yields the best ordering, mainly due to the 2nd step on nano-templated titanium. It will be interesting to see if multiple anodizations can eliminate the need of substrate polishing. Additionally, in-depth mechanical performances of nanopores and nanotubes need to be compared, simply because nanopores are structurally more robust than nanotubes (tend to bundle together and hence prone to fracture). Furthermore, it is worth noting that nanopores may reduce the drug loading abilities for the implant, as compared to nanotubes with significant inter-tube space. Another aspect with respect to nanotubes is the 'give and take' dependence between nanotube dimensions (directly co-relating to drug loading amounts and initial burst release amounts) and the mechanical stability, as studies have shown that smaller diameter/length means improved stability.

More recently advances have been made towards further augmenting the mechanics of TNTs based systems using various anodization modifications and other physical and chemical enhancements. Determined by nano-indentation, scratch and tensile tests and SEM, the most notable enhancements include Ti sputter coated on steel/alumina, annealing and the use of $(CH_3COO)_2Mg$ to enable sedimentation of fluoride ions. While clearly the outcomes indicate increments to mechanical stability as compared to conventional 'bare' nanotubes, whether or not such modified TNTs retain the implant applicability remains doubtful. For instance, whether drug loading/releasing functions can be integrated, or if the chemistry or topography remains unchanged (which may alter cell functions), or if such modifications leach ions post-implantation, largely remains unaddressed.

TNTs proposed for any application must be tested for stability concerns. For that matter, TNTs based implant modifications has been placed in the bone micro-environment, both in *ex vivo* and *in vivo* settings, to see if the nanotubes survives the mechanical handling, implantation surgery and the bone contact itself. While some success has been shown in this stability testing scenario, it has some limitations: most testing is short-term and no active load bearing conditions have been investigated post-implantation. To further

enhance this field of nano-engineered anodized implants it is crucial to study the mechanics at the bone-nanotube interface, such that it survives the micro-motion experienced during the bone growth and movement. Clearly, titania nanotubes are a promising orthopaedic and dental implant modification strategy with numerous studies establishing the enhanced bioactivity and therapeutic efficacy, however, to allow for easy integration into the current implant market, mechanical stability of these structures must be studied and enhanced to enable long-term success inside the compromised bone micro-environment.

References

1. Textor, M.; Sittig, C.; Frauchiger, V.; Tosatti, S.; Brunette, D. M. Properties and biological significance of natural oxide films on titanium and its alloys. In *Titanium in Medicine*; Brunette, D. M.; Tengvall, P.; Textor, M.; Thomsen, P., Eds.; Springer Berlin Heidelberg: Berlin, Heidelberg, 2001; pp 171-230.
2. Center for disease control *NCHS*. FastStats, Inpatient Surgery, Data for the U.S. Atlanta 2012.
3. Insights, B., The Top 10 orthopedic device companies: financial performance, research activities, and growth strategies. *Business Insights* 2010.
4. Kurtz, S. M.; Ong, K. L.; Schmier, J.; Mowat, F.; Saleh, K.; Dybvik, E.; Kärrholm, J.; Garellick, G.; Havelin, L. I.; Furnes, O. Future clinical and economic impact of revision total hip and knee arthroplasty. *J. Bone Joint Surg.* **2007**, *89*, 144-151.
5. Tobin, E. J. Recent coating developments for combination devices in orthopedic and dental applications: A literature review. *Adv. Drug Deliv. Rev.* **2017**, *112*, 88-100.
6. Junker, R.; Dimakis, A.; Thoneick, M.; Jansen, J. A. Effects of implant surface coatings and composition on bone integration: a systematic review. *Clin. Oral Implant. Res.* **2009**, *20*, 185-206.
7. Wennerberg, A.; Albrektsson, T.; Andersson, B.; Krol, J. A histomorghometric study of screw-shaped and removal torque titanium implants with three different surface topographies. *Clin. Oral Implant. Res.* **1995**, *6*, 24-30.
8. Wennerberg, A.; Hallgren, C.; Johansson, C.; Danelli, S. A histomorphometric evaluation of screw-shaped implants each prepared with two surface roughnesses. *Clin. Oral Implant. Res.* **1998**, *9*, 11-19.

9. Buser, D.; Schenk, R.; Steinemann, S.; Fiorellini, J.; Fox, C.; Stich, H. Influence of surface characteristics on bone integration of titanium implants. A histomorphometric study in miniature pigs. *J. Biomed. Mater. Res. A* **1991**, *25*, 889-902.
10. Hansson, S.; Norton, M. The relation between surface roughness and interfacial shear strength for bone-anchored implants. A mathematical model. *J. Biomech.* **1999**, *32*, 829-836.
11. Ma, Q. L.; Zhao, L. Z.; Liu, R. R.; Jin, B. Q.; Song, W.; Wang, Y.; Zhang, Y. S.; Chen, L. H.; Zhang, Y. M. Improved implant osseointegration of a nanostructured titanium surface via mediation of macrophage polarization. *Biomaterials* **2014**, *35*, 9853-9867.
12. García, A.; Reyes, C. Bio-adhesive surfaces to promote osteoblast differentiation and bone formation. *J. Dent. Res.* **2005**, *84*, 407-413.
13. Trisi, P.; Lazzara, R.; Rebaudi, A.; Rao, W.; Testori, T.; Porter, S. S. Bone-implant contact on machined and dual acid-etched surfaces after 2 months of healing in the human maxilla. *J. Periodontol.* **2003**, *74*, 945-956.
14. Mendonça, G.; Mendonça, D. B.; Aragao, F. J.; Cooper, L. F. Advancing dental implant surface technology–from micron-to nanotopography. *Biomaterials* **2008**, *29*, 3822-3835.
15. McNamara, L. E.; McMurray, R. J.; Biggs, M. J.; Kantawong, F.; Oreffo, R. O.; Dalby, M. J. Nanotopographical control of stem cell differentiation. *J. Tissue Eng.* **2010**, *1*, 120623.
16. Bauer, S.; Schmuki, P.; von der Mark, K.; Park, J. Engineering biocompatible implant surfaces: Part I: Materials and surfaces. *Prog. Mater. Sci.* **2013**, *58*, 261-326.
17. Kulkarni, M.; Mazare, A.; Gongadze, E.; Perutkova, Š.; Kralj-Iglič, V.; Milošev, I.; Schmuki, P.; Iglič, A.; Mozetič, M. Titanium nanostructures for biomedical applications. *Nanotechnology* **2015**, *26*, 062002.
18. Liu, H.; Webster, T. J. Nanomedicine for implants: a review of studies and necessary experimental tools. *Biomaterials* **2007**, *28*, 354-369.
19. Losic, D.; Simovic, S. Self-ordered nanopore and nanotube platforms for drug delivery applications. *Expert Opin. Drug Deliv.* **2009**, *6*, 1363-1381.
20. Roy, P.; Berger, S.; Schmuki, P. TiO_2 nanotubes: synthesis and applications. *Angew. Chem. Int. Ed.* **2011**, *50*, 2904-2939.
21. Tan, A.; Pingguan-Murphy, B.; Ahmad, R.; Akbar, S. Review of titania nanotubes: fabrication and cellular response. *Ceram. Int.* **2012**, *38*, 4421-4435.

22. Park, J.; Bauer, S.; von der Mark, K.; Schmuki, P. Nanosize and vitality: TiO_2 nanotube diameter directs cell fate. *Nano Lett.* **2007**, *7*, 1686-1691.
23. Gulati, K.; Ivanovski, S. Dental implants modified with drug releasing titania nanotubes: therapeutic potential and developmental challenges. *Expert Opin. Drug Deliv.* **2017**, *14*, 1009-1024.
24. Gulati, K.; Aw, M. S.; Findlay, D.; Losic, D. Local drug delivery to the bone by drug-releasing implants: perspectives of nano-engineered titania nanotube arrays. *Ther. Deliv.* **2012**, *3*, 857-873.
25. Zwilling, V.; Darque-Ceretti, E.; Boutry-Forveille, A.; David, D.; Perrin, M. Y.; Aucouturier, M. Structure and physicochemistry of anodic oxide films on titanium and TA6V alloy. *Surf. Interface Anal.* **1999**, *27*, 629-637.
26. Macak, J. M.; Sirotna, K.; Schmuki, P. Self-organized porous titanium oxide prepared in Na_2SO_4/NaF electrolytes. *Electrochim. Acta* **2005**, *50*, 3679-3684.
27. Gong, D.; Grimes, C. A.; Varghese, O. K.; Hu, W.; Singh, R.; Chen, Z.; Dickey, E. C. Titanium oxide nanotube arrays prepared by anodic oxidation. *J. Mater. Res.* **2001**, *16*, 3331-3334.
28. Albu, S. P.; Ghicov, A.; Aldabergenova, S.; Drechsel, P.; LeClere, D.; Thompson, G. E.; Macak, J. M.; Schmuki, P., Formation of double-walled TiO_2 nanotubes and robust anatase membranes. *Adv. Mater.* **2008**, *20*, 4135-4139.
29. Macak, J. M.; Tsuchiya, H.; Ghicov, A.; Yasuda, K.; Hahn, R.; Bauer, S.; Schmuki, P., TiO_2 nanotubes: self-organized electrochemical formation, properties and applications. *Curr. Opin. Solid. State. Mater. Sci.* **2007**, *11*, 3-18.
30. Taveira, L.; Macak, J.; Tsuchiya, H.; Dick, L.; Schmuki, P., Initiation and growth of self-organized TiO_2 nanotubes anodically formed in $NH_4F/(NH_4)_2SO_4$ electrolytes. *J. Electrochem. Soc.* **2005**, *152*, B405-B410.
31. Narayanan, R.; Kwon, T. Y.; Kim, K. H. TiO_2 nanotubes from stirred glycerol/NH_4F electrolyte: roughness, wetting behavior and adhesion for implant applications. *Mater. Chem. Phys.* **2009**, *117*, 460-464.
32. Thompson, G.; Furneaux, R.; Wood, G.; Richardson, J.; Goode, J. Nucleation and growth of porous anodic films on aluminium. *Nature* **1978**, *272*, 433-435.
33. Lee, K.; Mazare, A.; Schmuki, P. One-dimensional titanium dioxide nanomaterials: nanotubes. *Chem. Rev.* **2014**, *114*, 9385-9454.

34. Wei, W.; Berger, S.; Hauser, C.; Meyer, K.; Yang, M.; Schmuki, P. Transition of TiO_2 nanotubes to nanopores for electrolytes with very low water contents. *Electrochem. Commun.* **2010**, *12*, 1184-1186.
35. Valota, A.; LeClere, D.; Skeldon, P.; Curioni, M.; Hashimoto, T.; Berger, S.; Kunze, J.; Schmuki, P.; Thompson, G. Influence of water content on nanotubular anodic titania formed in fluoride/glycerol electrolytes. *Electrochim. Acta* **2009**, *54*, 4321-4327.
36. Albu, S. P.; Schmuki, P. Influence of anodization parameters on the expansion factor of TiO_2 nanotubes. *Electrochim. Acta* **2013**, *91*, 90-95.
37. Bedworth, R.; Pilling, N. The oxidation of metals at high temperatures. *J. Inst. Met.* **1923**, *29*, 529-582.
38. Macak, J.; Hildebrand, H.; Marten-Jahns, U.; Schmuki, P. Mechanistic aspects and growth of large diameter self-organized TiO_2 nanotubes. *J. Electroanal. Chem.* **2008**, *621*, 254-266.
39. Song, Y. Y.; Schmuki, P. Modulated TiO_2 nanotube stacks and their use in interference sensors. *Electrochem. Commun.* **2010**, *12*, 579-582.
40. Yoriya, S.; Paulose, M.; Varghese, O. K.; Mor, G. K.; Grimes, C. A. Fabrication of vertically oriented TiO_2 nanotube arrays using dimethyl sulfoxide electrolytes. *J. Phys. Chem. C* **2007**, *111*, 13770-13776.
41. Berger, S.; Kunze, J.; Schmuki, P.; Valota, A. T.; LeClere, D. J.; Skeldon, P.; Thompson, G. E. Influence of water content on the growth of anodic TiO_2 nanotubes in fluoride-containing ethylene glycol electrolytes. *J. Electrochem. Soc.* **2010**, *157*, C18-C23.
42. Zhu, W.; Liu, X.; Liu, H.; Tong, D.; Yang, J.; Peng, J. An efficient approach to control the morphology and the adhesion properties of anodized TiO_2 nanotube arrays for improved photoconversion efficiency. *Electrochim. Acta* **2011**, *56*, 2618-2626.
43. Berger, S.; Albu, S. P.; Schmidt-Stein, F.; Hildebrand, H.; Schmuki, P.; Hammond, J. S.; Paul, D. F.; Reichlmaier, S. The origin for tubular growth of TiO_2 nanotubes: a fluoride rich layer between tube-walls. *Surf. Sci.* **2011**, *605*, L57-L60.
44. Shimizu, K.; Kobayashi, K.; Thompson, G.; Skeldon, P.; Wood, G. Anodic oxide films on tantalum: incorporation and mobilities of electrolyte-derived species. *Phil. Mag. B* **1996**, *73*, 461-485.

45. Habazaki, H.; Fushimi, K.; Shimizu, K.; Skeldon, P.; Thompson, G. Fast migration of fluoride ions in growing anodic titanium oxide. *Electrochem. Commun.* **2007**, *9*, 1222-1227.
46. Zhang, Y.; Han, Y.; Zhang, L. Interfacial structure of the firmly adhered TiO_2 nanotube films to titanium fabricated by a modified anodization. *Thin Solid Films* **2015**, *583*, 151-157.
47. Macak, J. M.; Aldabergerova, S.; Ghicov, A.; Schmuki, P. Smooth anodic TiO_2 nanotubes: annealing and structure. *Phys. Status Solidi A* **2006**, *203*, R67-R69.
48. Prakasam, H. E.; Shankar, K.; Paulose, M.; Varghese, O. K.; Grimes, C. A. A new benchmark for TiO_2 nanotube array growth by anodization. *J. Phys. Chem. C* **2007**, *111*, 7235-7241.
49. Jarosz, M.; Pawlik, A.; Kapusta-Kołodziej, J.; Jaskuła, M.; Sulka, G. D. Effect of the previous usage of electrolyte on growth of anodic titanium dioxide (ATO) in a glycerol-based electrolyte. *Electrochim. Acta* **2014**, *136*, 412-421.
50. Proost, J.; Vanhumbeeck, J. F.; Van Overmeere, Q. Instability of anodically formed TiO_2 layers (Revisited). *Electrochim. Acta* **2009**, *55*, 350-357.
51. Gulati, K.; Santos, A.; Findlay, D.; Losic, D. Optimizing anodization conditions for the growth of titania nanotubes on curved surfaces. *J. Phys. Chem. C* **2015**, *119*, 16033-16045.
52. Sopha, H.; Hromadko, L.; Nechvilova, K.; Macak, J. M. Effect of electrolyte age and potential changes on the morphology of TiO_2 nanotubes. *J. Electroanal. Chem.* **2015**, *759*, 122-128.
53. Nelson, J.; Oriani, R. Stress generation during anodic oxidation of titanium and aluminum. *Corros. Sci.* **1993**, *34*, 307-326.
54. Zhao, L.; Mei, S.; Wang, W.; Chu, P. K.; Wu, Z.; Zhang, Y. The role of sterilization in the cytocompatibility of titania nanotubes. *Biomaterials* **2010**, *31*, 2055-2063.
55. Kummer, K. M.; Taylor, E. N.; Durmas, N. G.; Tarquinio, K. M.; Ercan, B.; Webster, T. J. Effects of different sterilization techniques and varying anodized TiO_2 nanotube dimensions on bacteria growth. *J. Biomed. Mater. Res. Part B Appl. Biomater* **2013**, *101*, 677-688.
56. Oh, S.; Brammer, K. S.; Moon, K. S.; Bae, J. M.; Jin, S. Influence of sterilization methods on cell behavior and functionality of osteoblasts cultured on TiO_2 nanotubes. *Mater. Sci. Eng. C.* **2011**, *31*, 873-879.

57. Junkar, I.; Kulkarni, M.; Drašler, B.; Rugelj, N.; Mazare, A.; Flašker, A.; Drobne, D.; Humpolíček, P.; Resnik, M.; Schmuki, P. Influence of various sterilization procedures on TiO_2 nanotubes used for biomedical devices. *Bioelectrochemistry* **2016**, *109*, 79-86.
58. Kulkarni, M.; Patil-Sen, Y.; Junkar, I.; Kulkarni, C. V.; Lorenzetti, M.; Iglič, A. Wettability studies of topologically distinct titanium surfaces. *Colloids Surf. B* **2015**, *129*, 47-53.
59. Yu, J.; Dai, G.; Cheng, B. Effect of crystallization methods on morphology and photocatalytic activity of anodized TiO_2 nanotube array films. *J. Phys. Chem. C* **2010**, *114*, 19378-19385.
60. Zhang, H.; Banfield, J. F. Phase transformation of nanocrystalline anatase-to-rutile via combined interface and surface nucleation. *J. Mater. Res.* **2000**, *15*, 437-448.
61. Yu, J.; Zhang, J. A simple template-free approach to TiO_2 hollow spheres with enhanced photocatalytic activity. *Dalton Trans.* **2010**, *39*, 5860-5867.
62. Aronsson, B. O.; Lausmaa, J.; Kasemo, B. Glow discharge plasma treatment for surface cleaning and modification of metallic biomaterials. *J. Biomed. Mater. Res. A* **1997**, *35*, 49-73.
63. Serro, A.; Saramago, B. Influence of sterilization on the mineralization of titanium implants induced by incubation in various biological model fluids. *Biomaterials* **2003**, *24*, 4749-4760.
64. Park, J. H.; Olivares-Navarrete, R.; Baier, R. E.; Meyer, A. E.; Tannenbaum, R.; Boyan, B. D.; Schwartz, Z. Effect of cleaning and sterilization on titanium implant surface properties and cellular response. *Acta Biomater.* **2012**, *8*, 1966-1975.
65. Att, W.; Hori, N.; Iwasa, F.; Yamada, M.; Ueno, T.; Ogawa, T. The effect of UV-photofunctionalization on the time-related bioactivity of titanium and chromium–cobalt alloys. *Biomaterials* **2009**, *30*, 4268-4276.
66. Seyeux, A.; Berger, S.; LeClere, D.; Valota, A.; Skeldon, P.; Thompson, G. E.; Kunze, J.; Schmuki, P. Influence of surface condition on nanoporous and nanotubular film formation on titanium. *J. Electrochem. Soc.* **2009**, *156*, K17-K22.
67. Fan, M.; La Mantia, F. Effect of surface topography on the anodization of titanium. *Electrochem. Commun.* **2013**, *37*, 91-95.
68. Lu, K.; Tian, Z.; Geldmeier, J. A. Polishing effect on anodic titania nanotube formation. *Electrochim. Acta* **2011**, *56*, 6014-6020.

69. Smith, Y. R.; Sarma, B.; Mohanty, S. K.; Misra, M. Single-step anodization for synthesis of hierarchical TiO_2 nanotube arrays on foil and wire substrate for enhanced photoelectrochemical water splitting. *Int. J. Hydrogen Energy* **2013**, *38*, 2062-2069.
70. Xing, J.; Li, H.; Xia, Z.; Chen, J.; Zhang, Y.; Zhong, L. Influence of substrate morphology on the growth and properties of TiO_2 nanotubes in HBF_4-based electrolyte. *Electrochim. Acta* **2014**, *134*, 242-248.
71. Kim, D.; Ghicov, A.; Schmuki, P. TiO_2 nanotube arrays: elimination of disordered top layers ("nanograss") for improved photoconversion efficiency in dye-sensitized solar cells. *Electrochem. Commun.* **2008**, *10*, 1835-1838.
72. Shin, Y.; Lee, S. Self-organized regular arrays of anodic TiO_2 nanotubes. *Nano Lett.* **2008**, *8*, 3171-3173.
73. Zhu, K.; Vinzant, T. B.; Neale, N. R.; Frank, A. J. Removing structural disorder from oriented TiO_2 nanotube arrays: reducing the dimensionality of transport and recombination in dye-sensitized solar cells. *Nano Lett.* **2007**, *7*, 3739-3746.
74. Hirakata, H.; Ito, K.; Yonezu, A.; Tsuchiya, H.; Fujimoto, S.; Minoshima, K. Strength of self-organized TiO_2 nanotube arrays. *Acta Mater.* **2010**, *58*, 4956-4967.
75. Li, S.; Zhang, G.; Guo, D.; Yu, L.; Zhang, W. Anodization fabrication of highly ordered TiO_2 nanotubes. *J. Phys. Chem. C* **2009**, *113*, 12759-12765.
76. Wang, F.; Liu, Y.; Dong, W.; Shen, M.; Kang, Z. Tuning TiO_2 photoelectrochemical properties by nanoring/nanotube combined structure. *J. Phys. Chem. C* **2011**, *115*, 14635-14640.
77. Zhang, Z.; Yu, Y.; Wang, P. Hierarchical top-porous/bottom-tubular TiO_2 nanostructures decorated with Pd nanoparticles for efficient photoelectrocatalytic decomposition of synergistic pollutants. *ACS Appl. Mater. Interfaces* **2012**, *4*, 990-996.
78. Rho, J. Y.; Tsui, T. Y.; Pharr, G. M. Elastic properties of human cortical and trabecular lamellar bone measured by nanoindentation. *Biomaterials* **1997**, *18*, 1325-1330.
79. Oliver, W. C.; Pharr, G. M. An improved technique for determining hardness and elastic modulus using load and displacement sensing indentation experiments. *J. Mater. Res.* **1992**, *7*, 1564-1583.
80. Crawford, G.; Chawla, N.; Das, K.; Bose, S.; Bandyopadhyay, A. Microstructure and deformation behavior of biocompatible TiO_2 nanotubes on titanium substrate. *Acta Biomater.* **2007**, *3*, 359-367.

81. Crawford, G.; Chawla, N.; Houston, J. Nanomechanics of biocompatible TiO_2 nanotubes by interfacial force microscopy (IFM). *J. Mech. Behav. Biomed. Mater.* **2009**, *2*, 580-587.
82. Kang, S. H.; Fang, T. H.; Chen, T. H.; Hsiao, Y. J.; Hong, Z. H.; Chuang, C. H.; Riccobono, L. Size effect on mechanical properties of TiO_2 capped nanotubes investigated using in situ transmission electron microscopy. *Microsys. Technol.* **2014**, *20*, 515-520.
83. Xu, Y.; Liu, M.; Wang, M.; Oloyede, A.; Bell, J.; Yan, C. Nanoindentation study of the mechanical behavior of TiO_2 nanotube arrays. *J. Appl. Phys.* **2015**, *118*, 145301.
84. Campanelli, L. C.; Bortolan, C. C.; da Silva, P. S. C. P.; Bolfarini, C.; Oliveira, N. T. C. Effect of an amorphous titania nanotubes coating on the fatigue and corrosion behaviors of the biomedical Ti-6Al-4V and Ti-6Al-7Nb alloys. *J. Mech. Behav. Biomed. Mater.* **2017**, *65*, 542-551.
85. Weszl, M.; Tóth, K. L.; Kientzl, I.; Nagy, P.; Pammer, D.; Pelyhe, L.; Vrana, N. E.; Scharnweber, D.; Wolf-Brandstetter, C.; Joób, Á. Investigation of the mechanical and chemical characteristics of nanotubular and nano-pitted anodic films on grade 2 titanium dental implant materials. *Mater. Sci. Eng. C.* **2017**, *78*, 69-78.
86. Baradaran, S.; Basirun, W.; Zalnezhad, E.; Hamdi, M.; Sarhan, A. A.; Alias, Y. Fabrication and deformation behaviour of multilayer Al_2O_3/Ti/TiO_2 nanotube arrays. *J. Mech. Behav. Biomed. Mater.* **2013**, *20*, 272-282.
87. Zalnezhad, E.; Hamouda, A.; Faraji, G.; Shamshirband, S. TiO_2 nanotube coating on stainless steel 304 for biomedical applications. *Ceram. Int.* **2015**, *41*, 2785-2793.
88. Hieda, J.; Niinomi, M.; Nakai, M.; Cho, K.; Mohri, T.; Hanawa, T. Adhesive strength of medical polymer on anodic oxide nanostructures fabricated on biomedical β-type titanium alloy. *Mater. Sci. Eng. C.* **2014**, *36*, 244-251.
89. Shokuhfar, T.; Arumugam, G. K.; Heiden, P. A.; Yassar, R. S.; Friedrich, C. Direct compressive measurements of individual titanium dioxide nanotubes. *ACS nano* **2009**, *3*, 3098-3102.
90. Chang, W. Y.; Fang, T. H.; Chiu, Z. W.; Hsiao, Y. J.; Ji, L. W. Nanomechanical properties of array TiO_2 nanotubes. *Micropor. Mesopor. Mat.* **2011**, *145*, 87-92.
91. Xiong, J.; Wang, X.; Li, Y.; Hodgson, P. D. Interfacial chemistry and adhesion between titanium dioxide nanotube layers and titanium substrates. *J. Phys. Chem. C* **2011**, *115*, 4768-4772.

92. Munirathinam, B.; Neelakantan, L. Role of crystallinity on the nanomechanical and electrochemical properties of TiO_2 nanotubes. *J. Electroanal. Chem.* **2016**, *770*, 73-83.
93. Rafieerad, A.; Bushroa, A.; Nasiri-Tabrizi, B.; Kaboli, S.; Khanahmadi, S.; Amiri, A.; Vadivelu, J.; Yusof, F.; Basirun, W.; Wasa, K. Toward improved mechanical, tribological, corrosion and in-vitro bioactivity properties of mixed oxide nanotubes on Ti–6Al–7Nb implant using multi-objective PSO. *J. Mech. Behav. Biomed. Mater.* **2017**, *69*, 1-18.
94. Wang, D.; Hu, T.; Hu, L.; Yu, B.; Xia, Y.; Zhou, F.; Liu, W. Microstructured arrays of TiO_2 nanotubes for improved photo-electrocatalysis and mechanical stability. *Adv. Funct. Mater.* **2009**, *19*, 1930-1938.
95. Schmidt-Stein, F.; Thiemann, S.; Berger, S.; Hahn, R.; Schmuki, P. Mechanical properties of anatase and semi-metallic TiO_2 nanotubes. *Acta Mater.* **2010**, *58*, 6317-6323.
96. Kar, A.; Raja, K.; Misra, M. Electrodeposition of hydroxyapatite onto nanotubular TiO_2 for implant applications. *Surf. Coat. Technol.* **2006**, *201*, 3723-3731.
97. Zazpe, R.; Prikryl, J.; Gärtnerova, V.; Nechvilova, K.; Benes, L.; Strizik, L.; Jäger, A.; Bosund, M.; Sopha, H.; Macak, J. M. Atomic layer deposition Al_2O_3 coatings significantly improve thermal, chemical, and mechanical stability of anodic TiO_2 nanotube layers. *Langmuir* **2017**, *33*, 3208-3216.
98. Yaghoubi, H.; Taghavinia, N.; Alamdari, E. K.; Volinsky, A. A. Nanomechanical properties of TiO_2 granular thin films. *ACS Appl. Mater. Interfaces* **2010**, *2*, 2629-2636.
99. Mayo, M.; Siegel, R.; Narayanasamy, A.; Nix, W. Mechanical properties of nanophase TiO_2 as determined by nanoindentation. *J. Mater. Res.* **1990**, *5*, 1073-1082.
100. Enache, C. S.; Schoonman, J.; van de Krol, R. Addition of carbon to anatase TiO_2 by n-hexane treatment—surface or bulk doping? *Appl. Surf. Sci.* **2006**, *252*, 6342-6347.
101. Van Raay, J.; Rozing, P.; Van Blitterswijk, C.; Van Haastert, R.; Koerten, H. Biocompatibility of wear-resistant coatings in orthopaedic surgery in vitro testing with human fibroblast cell cultures. *J. Mater. Sci. Mater. Med.* **1995**, *6*, 80-84.
102. Shivaram, A.; Bose, S.; Bandyopadhyay, A. Mechanical degradation of TiO_2 nanotubes with and without nanoparticulate silver coating. *J. Mech. Behav. Biomed. Mater.* **2016**, *59*, 508-518.

103. Aw, M. S.; Khalid, K. A.; Gulati, K.; Atkins, G. J.; Pivonka, P.; Findlay, D. M.; Losic, D. Characterization of drug-release kinetics in trabecular bone from titania nanotube implants. *Int. J. Nanomedicine* **2012**, *7*, 4883.
104. Rahman, S.; Gulati, K.; Kogawa, M.; Atkins, G. J.; Pivonka, P.; Findlay, D. M.; Losic, D. Drug diffusion, integration, and stability of nanoengineered drug-releasing implants in bone ex-vivo. *J. Biomed. Mater. Res. A* **2016**, *104*, 714-725.
105. Gulati, K.; Kogawa, M.; Prideaux, M.; Findlay, D. M.; Atkins, G. J.; Losic, D. Drug-releasing nano-engineered titanium implants: therapeutic efficacy in 3D cell culture model, controlled release and stability. *Mater. Sci. Eng. C.* **2016**, *69*, 831-840.
106. David, V.; Guignandon, A.; Martin, A.; Malaval, L.; Lafage-Proust, M. H.; Rattner, A.; Mann, V.; Noble, B.; Jones, D. B.; Vico, L. Ex vivo bone formation in bovine trabecular bone cultured in a dynamic 3D bioreactor is enhanced by compressive mechanical strain. *Tissue Eng. Part A* **2008**, *14*, 117-126.
107. Kaur, G.; Willsmore, T.; Gulati, K.; Zinonos, I.; Wang, Y.; Kurian, M.; Hay, S.; Losic, D.; Evdokiou, A. Titanium wire implants with nanotube arrays: a study model for localized cancer treatment. *Biomaterials* **2016**, *101*, 176-188.
108. von Wilmowsky, C.; Bauer, S.; Lutz, R.; Meisel, M.; Neukam, F. W.; Toyoshima, T.; Schmuki, P.; Nkenke, E.; Schlegel, K. A. In vivo evaluation of anodic TiO_2 nanotubes: an experimental study in the pig. *J. Biomed. Mater. Res. Part B Appl. Biomater*. **2009**, *89*, 165-171.
109. Bjursten, L. M.; Rasmusson, L.; Oh, S.; Smith, G. C.; Brammer, K. S.; Jin, S. Titanium dioxide nanotubes enhance bone bonding in vivo. *J. Biomed. Mater. Res. A* **2010**, *92*, 1218-1224.
110. Choi, S. H.; Cha, J. Y.; Joo, U. H.; Hwang, C. J. Surface changes of anodic oxidized orthodontic titanium miniscrew. *Angle Orthod.* **2011**, *82*, 522-528.
111. Jang, I.; Shim, S. C.; Choi, D. S.; Cha, B. K.; Lee, J. K.; Choe, B. H.; Choi, W. Y. Effect of TiO_2 nanotubes arrays on osseointegration of orthodontic miniscrew. *Biomed. Microdevices* **2015**, *17*, 76.

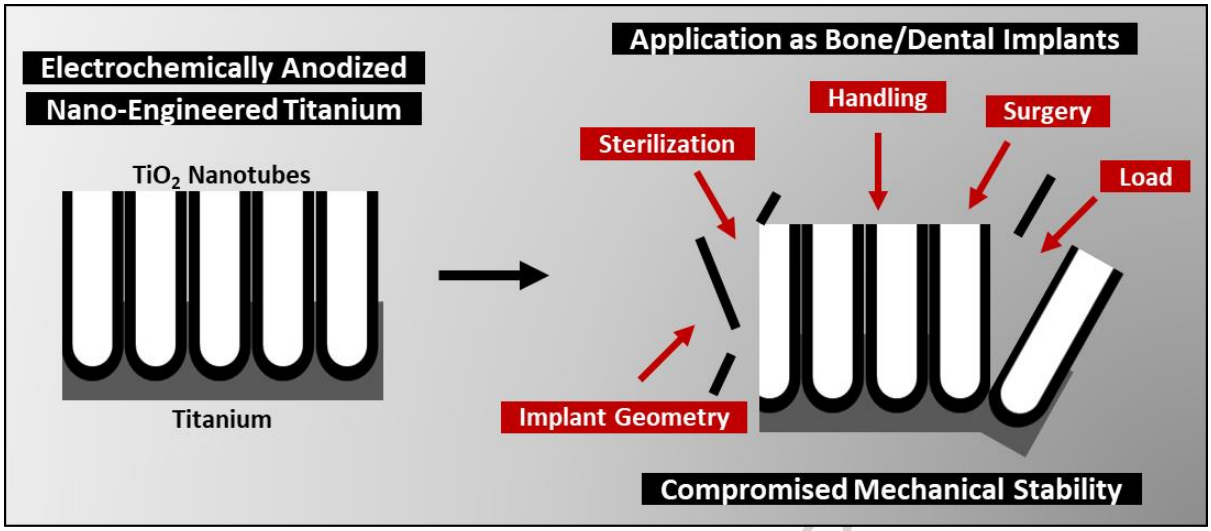

Graphical abstract

Highlights

- Titania nanotubes (TNTs) modified implants enable enhanced bioactivity and local drug delivery.
- The mechanical stability of TNTs at nanotube-titanium and nanotube-bone interface is crucial but remains under-explored.
- We discuss the mechanical stability of TNTs/Ti implants towards achieving desirable performances, without the risk of delamination or damage.